Ocean and Coastal Management 200 (2021) 105462

Contents lists available at ScienceDirect

Ocean and Coastal Management

journal homepage: http://www.elsevier.com/locate/ocecoaman

Evidence of localised upwelling in Pemba Channel (Tanzania) during the southeast monsoon

Stuart C. Painter [a,*], Baraka Sekadende [b], Angelina Michael [c,e], Margaux Noyon [d], Salome Shayo [b], Brian Godfrey [d], Mtumwa Mwadini [c], Margareth Kyewalyanga [c]

[a] National Oceanography Centre, Southampton, UK
[b] Tanzania Fisheries Research Institute, Dar es Salaam, Tanzania
[c] Institute of Marine Sciences, University of Dar es Salaam, Tanzania
[d] SA-UK Bilateral Chair: Ocean Science & Marine Food Security, Nelson Mandela University, Port Elizabeth, South Africa
[e] College of Natural and Mathematical Sciences, University of Dodoma, Tanzania

ARTICLE INFO

Keywords:
East african coastal current
Pemba channel
Upwelling
Western indian ocean
Biogeochemistry
Phytoplankton
Coccolithophores
Gephyrocapsa

ABSTRACT

Oceanographic and biogeochemical observations collected in Pemba Channel, a deep-water (800 m) channel separating Pemba Island from mainland Tanzania, during the South East monsoon indicate the presence of active upwelling along the western edge of Pemba Island. Surface salinity values, nutrient concentrations and the presence of coccolithophore species previously reported from the mid to lower euphotic zone all suggest upwelling from at least 80–100 m depth. The surface waters of the channel were characterised with low NO_3^-:PO_4^{3-} (0.68:1) and NO_3^-:Si (0.04:1) ratios far below the Brzezinski-Redfield ratio indicating the presence of N-limitation and the possibility that these waters may be susceptible to anthropogenic N inputs. Surface NO_3^- concentrations averaged 0.09 ± 0.10 μmol L^{-1} but increased to 0.5 μmol L^{-1} in the centre of upwelling where coincidentally both integrated nutrient concentrations and surface POC/PON pools were approximately 2-fold higher than the channel average. Despite its significance for local productivity upwelling is tentatively estimated, via stoichiometric assumptions, to enhance local productivity by only 20%. The modest productivity response to upwelling may be explained by picoplankton (0.2–2 μm) dominance of the phytoplankton community with this size-class representing ~80% of total chlorophyll-*a*. Nevertheless, important spatial variability was identified in larger size fractions and supported by taxonomic analyses with indications that the distribution of *Chaetoceros* spp. alone may be particularly relevant for understanding the variability in larger (>20 μm) chlorophyll-*a* size fractions. The location of upwelling has previously been shown to host large concentrations of small pelagic fish thus management of this regionally important resource would benefit from additional investigation of the underlying physical mechanism driving upwelling and subsequently how trophic interactions and ecosystem productivity are influenced.

1. Introduction

Sustainable management of the natural ocean resources of the Western Indian Ocean is increasingly recognised as being central to the socio-economic future of the region (Obura et al., 2017). It is estimated that around 60 million people, approximately one-third of the regional population, live within 100 km of a coastline with many dependent upon the ocean for employment and for their primary source of protein (van der Elst et al., 2005; Taylor et al., 2019). There is however, growing awareness that historic under sampling of the Western Indian Ocean is likely to impede effective management decision making (Van der Elst and Everett 2015).

This is particularly true for that section of the East African coastline influenced by the East African Coastal Current (EACC), where extant oceanographic observations are limited, biogeochemical measurements are sparse, and many key results are now several decades old, difficult to access, contradictory, or of questionable quality (Painter 2020). Such a situation hampers efforts to effectively and sustainably manage marine resources, complicates efforts to produce regional environmental syntheses and leaves many basic questions about the marine environment

* Corresponding author.
E-mail address: stuart.painter@noc.ac.uk (S.C. Painter).

https://doi.org/10.1016/j.ocecoaman.2020.105462
Received 13 May 2020; Received in revised form 28 October 2020; Accepted 22 November 2020
Available online 7 December 2020

and how it may respond in future unanswerable.

The region influenced by the EACC (~3–11°S) formally lies within the Exclusive Economic Zones of Tanzania and Kenya. Swallow et al. (1991), determined that the core of the EACC lies seaward of the narrow continental shelf but that the current's influence is negligible beyond 200 km offshore. Along the coastline of Tanzania complex bathymetry allows the EACC to approach close to the mainland. The Pemba Channel (~5.2°S, 39.3°E), separates the island of Pemba from the East African mainland and is one of three narrow seaways found along the Tanzanian coast. Together with the neighbouring Zanzibar Channel (~6°S) near Unguja (Zanzibar) Island and Mafia Channel (~8°S) near Mafia Island, these seaways provide important foci for artisanal and subsistence fishing communities due to the sheltered waters they offer and the ease of access for traditional fishing vessels. Pemba Channel is unique amongst these three seaways in that it is the only deep water channel (~800 m deep, ~40 km wide) found along the Tanzanian coast and is thus suggested to have an important role in bringing nutrient rich intermediate depth oceanic waters from the open Western Indian Ocean close to the coast, most likely facilitated by the limb of the EACC that passes through the Pemba Channel (Semba et al., 2019). Upwelling of nutrient rich water along the Tanzanian coast has long been suggested (Bakun et al., 1998), and could be significant for primary production and hence for local fisheries, but until recently direct evidence for upwelling was equivocal or wrongly attributed. Jebri et al. (2020) have now identified contrasting nutrient enrichment mechanisms at work during different monsoon seasons. Whilst traditional wind-driven upwelling was found to explain enhanced phytoplankton biomass along the coast during the northeast monsoon, the larger biological response during the southeast monsoon results from the dynamic uplift of isopycnal and nutrient isopleths as the EACC approaches the coast coupled with horizontal advection of nutrients by stronger southeasterly winds.

Environmental conditions within Pemba Channel and along the Tanzanian coast are of interest due to the socioeconomic and food security significance resident small pelagic fish populations play (Anderson and Samoilys 2016; Taylor et al., 2019; Sekadende et al., 2020). The channel and the wider EACC influenced region are also unique for a tropical coastal ecosystem as significant monsoon driven seasonality impacts the upper ocean making the region unlike comparable tropical coastal ecosystems of the Atlantic and Pacific Oceans (Newell 1957, 1959; Leetmaa 1972; Wyrtki 1973; Harvey 1977; Bryceson, 1982; McClanahan 1988). Consequently, adoption of management practices from elsewhere may not be appropriate and improved knowledge of the environmental conditions in Pemba Channel is thus central to improved environmental and fisheries management. Here oceanographic and biogeochemical observations from Pemba Channel made during the SE monsoon period are presented to complement ongoing efforts to understand and manage these waters more effectively.

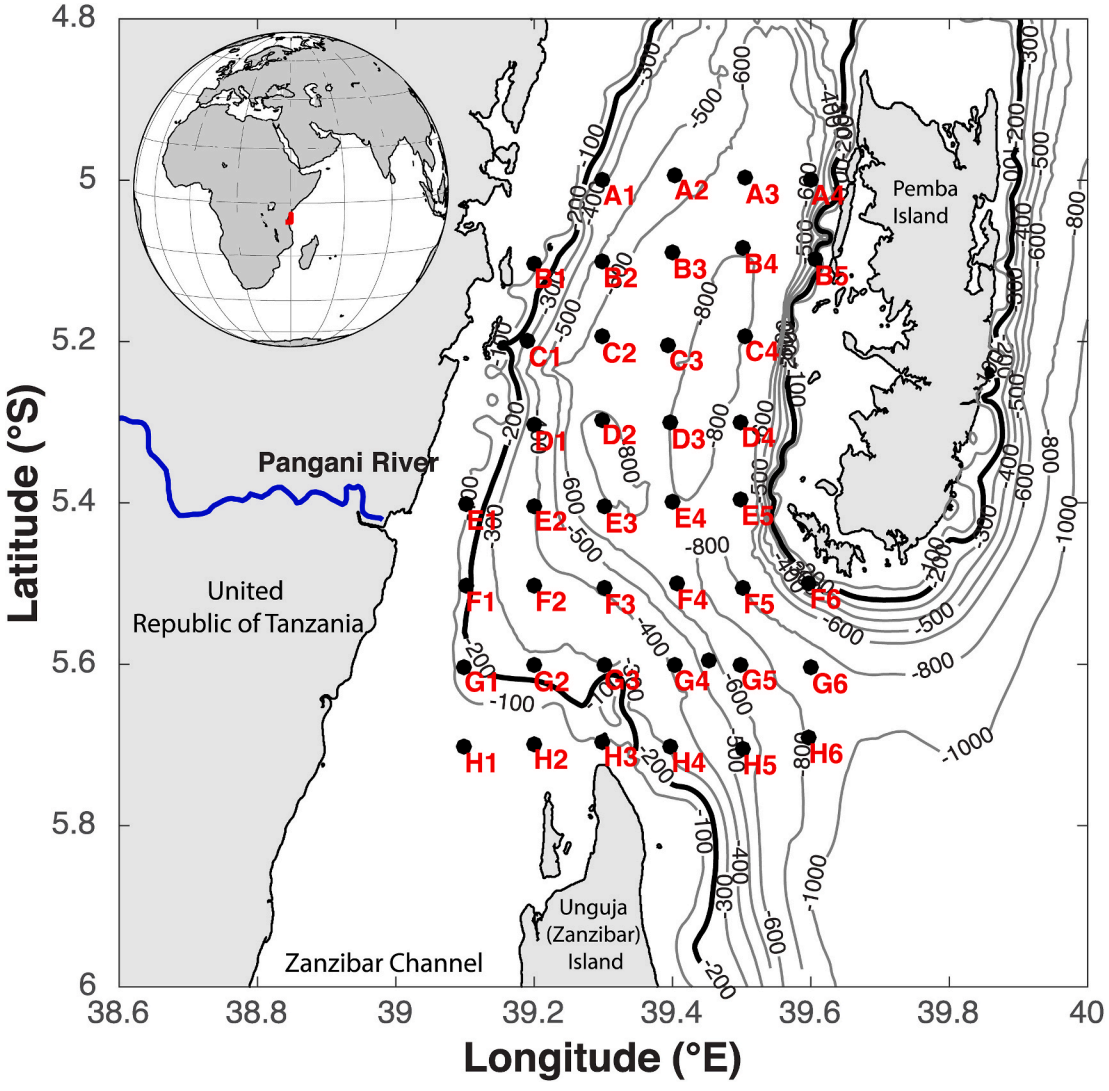

Fig. 1. Map showing the study location in the Western Indian Ocean (inset image) and sampling stations within Pemba Channel.

2. Methods

2.1. Oceanographic survey

A 10-day research cruise through the Pemba Channel was conducted between June 30th and July 9th, 2019 using the M.Y. *Angra Pequena*, a 24 m expedition yacht fitted with a Palfinger crane on the foredeck allowing deployment of a small CTD system to ~500 m. Maximum sampling depths ranged from 50 m to 500 m depending upon local bathymetry and maximum wire out (500 m). In the deep waters of the central channel sampling to 500 m was often challenging due to the strength of the northward flowing EACC and maximum sampling depths were variable. Forty stations were sampled with an approximate horizontal spacing of ~11 km over the slopes and deeper parts of the channel (Fig. 1). Vertical profiles of temperature, salinity, chlorophyll-*a* fluorescence and PAR were made using an SBE19+ CTD system equipped with a SBE55 rosette sampler fitted with 6 x 6 L Niskin bottles to allow collection of seawater at standard sampling depths of 5, 25, 50, 75, 100 and 150 m. At shallow slope stations modified sampling depths were chosen based on water depth.

2.2. Hydrographic characterization

Mixed layer depths and mean mixed layer properties were calculated for each CTD profile using the density based algorithm described by Holte and Talley (2009). A seasonal context for the cruise data was obtained by comparison to the Argo derived mixed layer climatology of Holte et al. (2017) (http://mixedlayer.ucsd.edu). Passage of Argo floats through the Pemba Channel is comparatively rare and in order to construct a mean annual cycle of mixed layer characteristics from the climatology the climatological monthly mixed layer depth was averaged for a 2° by 2° region (4.5–6.5°S, 38.5–40.5°E). This region incorporates deep ocean waters to the east of Pemba Island more strongly influenced by the EACC than the channel itself but the result is considered representative of regional conditions. Hydrographic results are reported using TEOS-10 (UNESCO 2010), except where comparison to older literature warrants use of EOS-80 (UNESCO 1981).

2.3. Chlorophyll-a

Bulk chlorophyll-*a* concentrations were measured using the fluorometric method of Welschmeyer (1994). For each sample 250 mL of seawater was filtered onto 25 mm Whatman glass fibre filters (GF/F; ~0.7 μm pore size) under gentle vacuum. Pigment extraction was conducted in 6 mL of 90% acetone in the dark at 4 °C, over a subsequent 18–20 h period and sample fluorescence was measured on a Turner trilogy fluorometer calibrated against a fresh chlorophyll-*a* standard (Sigma, UK). Concentrations are reported in units of mg m^{-3}.

Size fractionated chlorophyll-*a* concentrations were obtained by filtration of replicate 250 mL samples onto 2 μm, 10 μm and 20 μm polycarbonate membrane filters with extraction and analysis as described above for bulk chlorophyll-*a* samples. Chlorophyll-*a* concentrations are reported for four size fractions (0.7–2 μm, 2–10 μm, 10–20 μm and >20 μm) and are based on calculation of numerical differences between the size fractions.

2.4. Nutrients

Nutrient samples were collected at all stations and at all sampled depths. Samples were collected in 50 mL centrifuge tubes and pasteurised at 80 °C for 2 h (Daniel et al., 2012) before storage in dark containers and shipment to the UK for analysis. Samples were analysed for silicate (Si), phosphate (PO_4^{3-}), total nitrate ($NO_3^- + NO_2^-$) and nitrite (NO_2^-) content using a Seal Analytics Quaatro autoanalyzer, established methods (Hydes et al., 2010) and certified reference materials (Kanso, Japan). Concentrations are reported in units of μmol L^{-1}. The nitracline was determined as the depth where the total nitrate concentration reached 1 μmol L^{-1} using interpolated vertical profiles (due to the low vertical sampling resolution).

2.5. Particulate organic carbon and nitrogen

Particulate organic carbon (POC) and nitrogen (PON) concentrations and the associated isotopic content were determined via coupled elemental analysis and mass spectrometry. One litre seawater samples were filtered under vacuum onto ashed (450 °C, >4 h) GFF filters and rinsed with a pH buffered solution (~pH 8) of pure water (1 L pure water plus 800 μl of ammonium solution) before filters were placed in 2 mL cryo-vials and dried overnight at 40 °C. In the laboratory, filters were extracted and fumed with concentrated HCl to remove inorganic carbon before being dried again overnight at 40 °C and then packaged into tin capsules for analysis. Concentrations are reported in units of μmol C L^{-1} or μmol N L^{-1}, while the isotopic content is reported using the delta notation ($\delta^{13}C$ and $\delta^{15}N$) and in units of per mil (‰).

2.6. Irradiance

Measurements of surface irradiance (PAR, 400–700 nm) were made by installation of a biophysical Licor PAR sensor on the bridge top, whilst subsurface measurements were made with a Satlantic PAR sensor attached to the CTD package. Water column attenuation coefficients (Kd) were calculated for each cast as the slope of the natural log transformed PAR data. Subsurface sampling depths as a function of surface irradiance, and the depth of the euphotic zone, were estimated from the cruise mean attenuation coefficient.

2.7. Phytoplankton community

Surface water samples were collected at most, but not all, stations for the primary purpose of coccolithophore identification and enumeration, though diatoms were also identified as a secondary activity. A single 500 mL seawater sample was collected from the surface Niskin bottle (nominal depth 5 m) and filtered on to a 25 mm diameter 0.8 μm pore-size polycarbonate filter (Whatman). Samples collected in this manner are considered representative of the upper euphotic zone (>10% surface irradiance). After filtration filters were placed into petri slides, oven dried at ~40 °C for 24 h, and then stored for subsequent analysis.

In the laboratory a small piece of filter (~1 cm^2) was cut out and fixed to an aluminium stub before being sputter coated with gold. The coccolithophore assemblages were examined with a Zeiss (LEO) 1450 V P scanning electron microscope (SEM) at a magnification of 5000× across a grid of 15 × 15 fields of view (FOV). Identification of coccolithophore species relied upon the classification schemes of Cros and Fortuno (2002), Young et al. (2003) and Nannotax3 (www.mikrotax.org/Nannotax3/), whilst diatom identification followed Round et al. (1990) and Hasle and Syvertsen (1997). Due to many coccolithophore species being present at low abundances and making only minor contributions to total coccolithophore abundance most taxa were grouped by genus (see Appendix A). Aggregates of identical coccoliths and collapsed coccospheres were included in to the coccosphere counts. Coccolithophore abundances (coccospheres L^{-1}) were calculated as.

2.8. Coccolithophore abundance = F x C/A x V [1]

Where F is the total sample filtration area (mm^2), C is the number of counted coccospheres (per species or genus), A is the total area represented by the SEM micrographs (mm^2; i.e. the counted area), and V is the volume filtered (in litres). Based on the magnification, volume filtered and numbers of fields of view examined the volume counted per samples ranged from 1.39 to 1.61 mL.

The ecological indices of species richness (S), which is simply the total number of species per sample, Shannon-Wiener diversity index

(H′), which provides insight into the extent of species homogeneity between samples, and Pielou's eveness index (J′), which measures how evenly the count data were distributed amongst the species present, were calculated as described in Magurran (2004).

$$H' = -\sum \frac{n_i}{N} \ln \frac{n_i}{N} \quad [2]$$

where for each sample n_i is the number of individuals of each taxon, and N is the total number of all individuals.

$$J' = \frac{H'}{ln(S)} \quad [3]$$

where H′ is obtained from equation 2 and S is the number of species per sample (species richness).

Numerous small diatom cells were observed throughout the samples and a brief summary is presented here, though they were not the primary focus of study. Previously, Moto et al. (2018) noted that diatoms typically account for ~70% of larger phytoplankton species in these waters. As acid washing of samples prior to gold coating would have impacted the coccolithophore analysis it was not always possible to obtain definitive taxonomic identification of all diatom cells. Information on the microplankton community (>20 μm) present during this study will be presented elsewhere whilst more general descriptions for these waters can be found in Moto et al. (2018), Lugomela and Semesi (1996), Lugomela (2013) and references therein.

2.9. Multivariate analysis

The coccolithophore assemblage was analysed using multivariate ordination via the *Vegan* package in R (R Core Team, 2016; Oksanen et al., 2019). Due to low abundances individual species were grouped before analysis as described in Table A1. Bray-Curtis dissimilarities were calculated using log (x+1) transformed coccolithophore abundances and clusters of stations identified using non-metric multidimensional scaling (nMDS). Two dimensions were calculated with acceptable stress (<0.2; Legendre and Legendre, 1998) before the *envfit* function was used to fit select environmental data (salinity, temperature, Chl-a, turbidity, NO_3, Si, PO_4) to the nMDS ordination to identify relationships between the coccolithophore community and the environmental variables.

2.10. Zooplankton biovolume

Zooplankton samples were collected at each station using 200 μm bongo nets fitted with a Star-Oddi depth sensor and a flow meter, and hauled obliquely from ~200 m to the surface (max depth range 145–259 m) or from 10 m above the sea bed to the surface at shallower stations. Samples were preserved in 4% formaldehyde final concentration. Samples were subsequently settled for 24–48 h in graduated measuring cylinders to obtain an indication of biovolume which is reported here as an average biovolume per filtered volume of water and in integrated form.

2.11. Remote sensing datasets

MODIS-Aqua data for the period 2002–2019 were downloaded from the NASA Ocean Color repository (https://oceancolor.gsfc.nasa.gov). Level-3 mapped data (reprocessing v2018.0) with a 4 km spatial resolution and an 8-day composite temporal resolution were used to produce the mean annual cycles of chlorophyll-*a*, SST, particulate inorganic carbon, and irradiance (PAR 400–700 nm wavelengths) over the deeper waters of the Pemba Channel (5–5.7°S, 39.3–39.6°E) in order to provide context for the cruise measurements.

3. Results

3.1. Hydrography

Temperature and salinity profiles were evaluated with reference to regional water masses and characteristic TS profiles (Fig. 2). The CTD data fit closely to the mean EACC regional TS profile reported by Painter (2020) and World Ocean Database hydrographic data holdings but both differed slightly from the mean profile for the EACC region reported by Schott and McCreary (2001), which reported higher salinity values but was otherwise similar.

Across the sampled depth ranges temperature ranged from a minimum of 9.6 °C to a maximum of 27.4 °C, whilst salinity ranged from 34.835 to 35.36 (on the PSS-78 scale) (35.003–35.528 g kg^{-1} under TEOS-10). A salinity maximum, indicative of South Indian Central water (SICW), was clearly present along each transect spanning the width of the channel and on average was located at a depth of 153 ± 14 m and located beneath Tropical Surface Water (TSW) (Fig. 3).

3.2. Surface PAR and irradiance

Maximum daily (PAR) photon flux measured at the bridge top ranged from 1465 to 2132 μmol photons m^{-2} s^{-1}. Daily light integrals averaged 35.3 ± 8.77 mol s photons m^{-2} d^{-1} over the sampling period but varied from a daily minimum of 18.96 mol s photons m^{-2} d^{-1} to a daily maximum of 44.46 mol s photons m^{-2} d^{-1}. Daily light integrals approximately halved over the sampling period due to steadily increased cloud cover.

Water column attenuation coefficients (K_d) ranged from 0.037 to 0.094 m^{-1}, and for the entire dataset averaged 0.051 ± 0.011 m^{-1}. Attenuation estimates from several shallow stations (F1, G1, H1–H3) however, exceeded 0.0600 m^{-1} and therefore skewed the overall cruise mean. Exclusion of these five shallow stations, where sediment resuspension or possibly discharge from the Pangani River may have impacted the attenuation coefficient, resulted in a lower mean attenuation of 0.047 ± 0.005 m^{-1} (range 0.037–0.058 m^{-1}) and better agreement with typical values from low latitude open ocean waters (Kirk 2010). The mean depth of the euphotic zone (1% surface PAR), was thus 97 m extending to 146 m for the 0.1% isolume.

3.3. Mixed layer depth

For a 2°-by-2° region (4.5–6.5°S, 38.5–40.5°E) centred on the Pemba Channel the Argo mixed layer climatology indicated typical mixed layer depths ranging from ~30 m during the NE monsoon months (Dec–Mar) to ~70 m during the SE monsoon months (Jun–Sep) (Fig. 4), in keeping with existing descriptions of mixed layer seasonal behaviour (e.g. (Hartnoll 1974)). Mean mixed layer conditions are presented in Table 1. The mixed layer depth measured during the cruise in June/July was highly variable, ranging from 9 to 123 m (Fig. 4) which was shallower than implied by the climatology (67 m for July). Average mixed layer temperatures ranged from 26.50 to 27.10 °C, and could be up to 1 °C warmer than implied by the climatology, whilst S_A ranged from 35.137 to 35.330 g kg^{-1} and was generally lower than indicated by the climatology (Fig. 4). Mixed layer densities ranged from 22.712 to 22.868 kg m^{-3}.

3.4. Surface hydrography

Surface (5 m) measurements were interpolated and contoured in order to better understand the spatial variability within the channel (Fig. 5). A prominent east-west thermal gradient was evident with cooler waters (<26.9 °C) located in the eastern half of the channel. Warmer waters (>26.9 °C) were found in shallower areas in the western half of the channel and there is a suggestion of a warm water influence emanating from the shallow Zanzibar Channel and mainland shelf

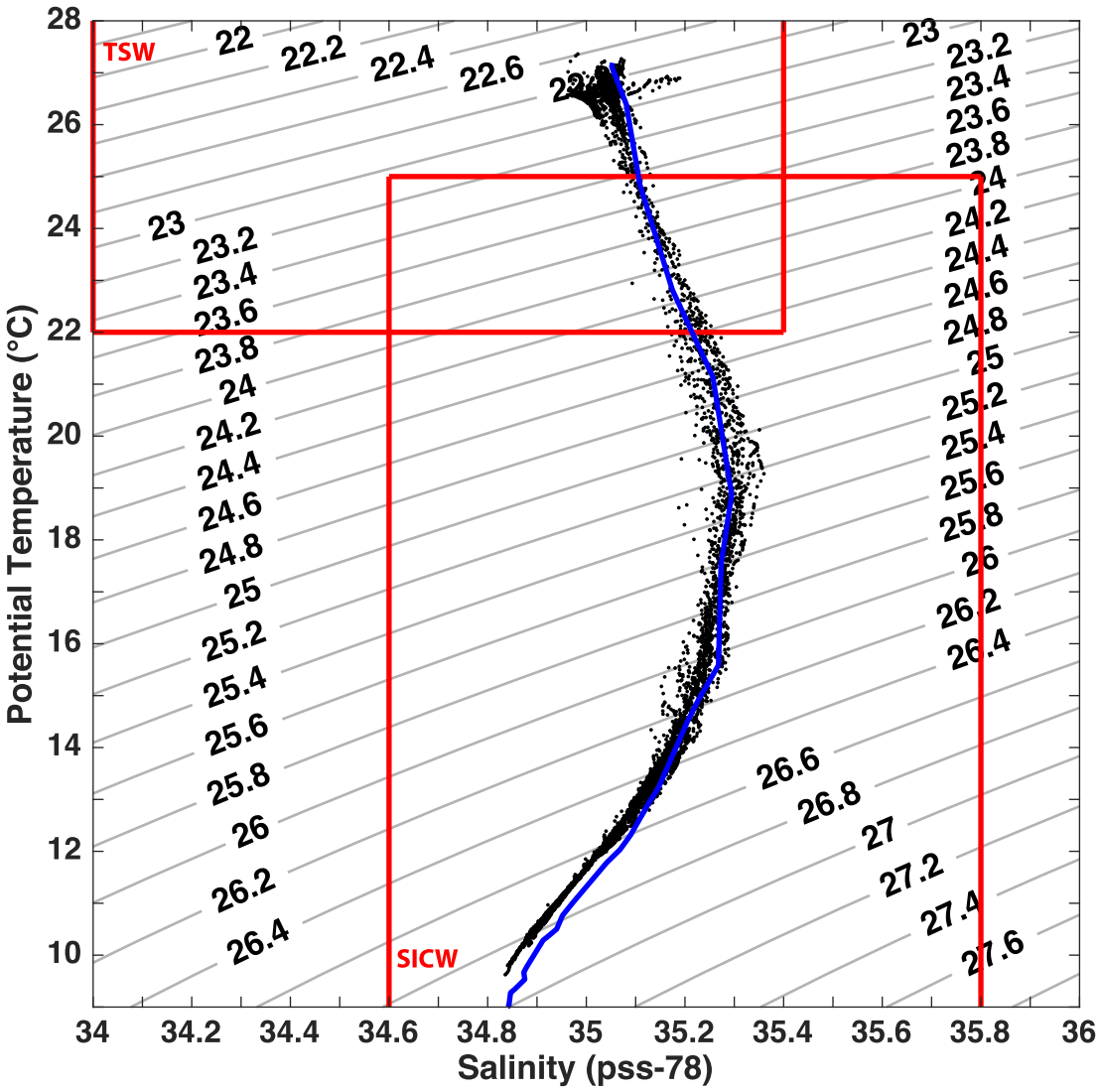

Fig. 2. Temperature-Salinity plot of the CTD data (black dots) in relation to a recent reanalysis of historical data for the EACC region (blue line; Painter 2020). Two key regional water masses indicated by the red boxes are South Indian Central Water (SICW) and Tropical Surface Water (TSW). Note that this data presentation uses EOS-80 to be consistent with the historical reanalysis reported by Painter (2020). (For interpretation of the references to colour in this figure legend, the reader is referred to the Web version of this article.)

regions. Surface salinity was less spatially variable and no shelf-slope gradients could be identified. No salinity signature could be associated with the Pangani River which discharges at approximately 5.4°S (5° 24′S). Spatial variation in the surface density field closely followed spatial variability in temperature.

3.5. Nutrients

Surface nutrient concentrations were low but measurable with traditional micromolar techniques (Fig. 5; Table 1). Surface nitrate concentrations ranged from <0.02 to 0.59 μmol L^{-1}, phosphate concentrations ranged from 0.10 to 0.18 μmol L^{-1}, and silicate concentrations ranged from 2.05 to 3.47 μmol L^{-1}.

Surface waters were rich in Si, and comparatively rich in P, relative to inorganic N. Shallow inshore stations at the western ends of lines E to H suggest a prominent Si source from the Zanzibar Channel or more likely from the shelf sediments (Fig. 5). Phosphate distributions indicated enrichment of surface waters at several localised positions, including off Nungwi (northern tip of Unguja Island), at station D4 along the western coast of Pemba Island and at station G6 at the entrance to the Pemba Channel. There was a tendency towards higher PO_4^{3-} concentrations (>0.12 μmol L^{-1}) in eastern Pemba Channel (western coastline of Pemba Island) but this east-west gradient is very slight. Nitrate distributions revealed a single dominant site of surface enrichment at station D4 with a secondary and minor enrichment, possibly as a result of an island wake effect, downstream of Unguja Island along the shelf break. The surface waters of Pemba Channel were otherwise severely N limited when compared to the Redfield ratio (N:P:Si = 16:1:15), a conclusion reinforced by the low average $NO_3^- + NO_2^-$:PO_4^{3-} (N:P) ratio of 0.68:1 calculated for these waters (note however that the influence of ammonium on the N:P ratio is not considered). Similarly, the low mean N:Si value of 0.04 ± 0.04 also illustrates the severity of N limitation in these waters. A mean Si:P value of 19.40 ± 2.96 was also calculated.

Deep nutriclines were evident for all nutrients (Figs. 6 and 7). The mean depth of the nitracline was 90 ± 20 m (range 30–151 m). Water samples collected from 400 m depth at a station midway between station G4 and G5 (Fig. 1) indicated nutrient concentrations of 21.5 μmol NO_3^- L^{-1}, 1.44 μmol PO_4^{3-} L^{-1} and 16.1 μmol Si L^{-1}. The cruise mean nitracline gradient, a useful metric for calculating vertical diffusive fluxes, was 169.7 ± 63.1 μmol m^{-4} but stations located close to the Zanzibar Channel and mainland shelf areas (Station E1, G1, H1–H3), and which

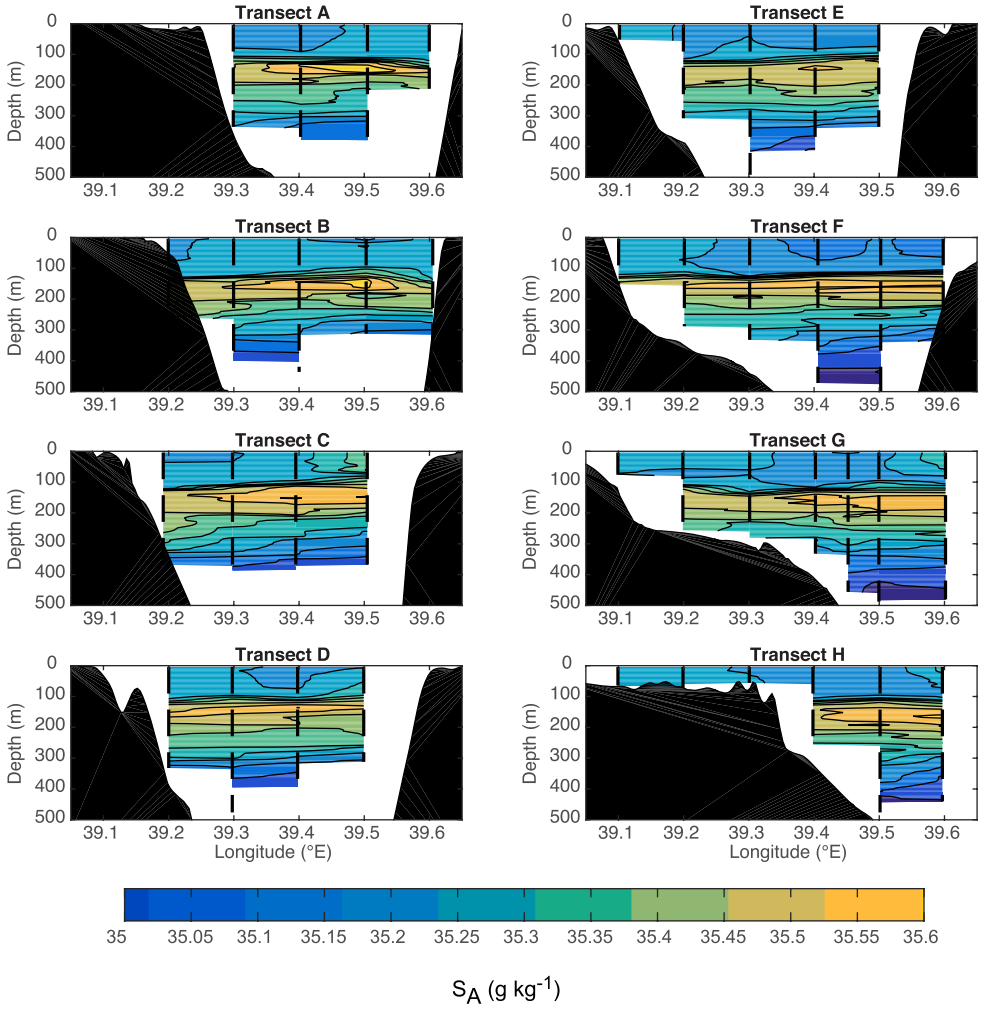

Fig. 3. Contoured cross sections of Absolute Salinity presented by transect, see Fig. 1 for positions of each transect.

were typically shallower than the cruise mean nitracline depth, exhibited weaker gradients (mean 33.2 ± 25.6 μmol m^{-4}) distorting the overall cruise mean. Exclusion of these shallow stations resulted in an average nitracline gradient for the channel of 188.7 ± 38.1 μmol m^{-4} which when coupled with a typical oceanic diffusivity of 0.1 cm^2 s^{-1} suggests a vertical diffusive NO_3^- flux of order ~163 ± 33 μmol NO_3^- m^{-2} d^{-1}.

Integrated (0–150 m) nutrient pools ranged from 80.2 to 755.8 mmol m^{-2}, 20.0–64.2 mmol m^{-2} and 364.6–785.5 mmol m^{-2} for nitrate, phosphate and silicate respectively. At shallow inshore stations (E1, G1, H1, H2, H3) where the integration depth was <75 m nutrient concentrations ranged from 1.5 to 17.4 mmol m^{-2}, 6–9.7 mmol m^{-2} and 144.5 to 222 0.6 mmol m^{-2} for nitrate, phosphate and silicate respectively. Integrated nutrient pools varied along each transect (Table 2).

3.6. Chlorophyll-*a*

Surface (5 m) total chlorophyll-*a* concentrations ranged from 0.14 to 0.92 mg m^{-3} and averaged 0.39 ± 0.13 mg m^{-3}. The highest surface concentration of 0.92 mg m^{-3} was obtained at station H3 (~120 m water depth) whilst the lowest concentration of 0.14 mg m^{-3} was measured at station A1 (~365 m water depth) (Fig. 5). There was no correlation between water depth and surface total chlorophyll-*a* concentration.

Chlorophyll-*a* concentrations increased with depth at all stations due to the presence of a broad subsurface chlorophyll-*a* maximum (Fig. 6). The subsurface distribution of chlorophyll-*a* was patchy and variable along each transect but generally restricted to the upper 100 m of the water column and thus above the thermocline (Figs. 6 and 8). Based on collected seawater samples maximum subsurface chlorophyll-*a* concentrations ranged from 0.34 to 0.95 mg m^{-3} (mean 0.51 ± 0.12 mg m^{-3}), thus on average chlorophyll-*a* concentrations at the subsurface maxima were around 30% higher than mean surface concentrations. The depth of the maximum varied from 15 to 75 m (mean 47 ± 20 m) but as this is based upon fixed depth sampling it should be viewed as indicative only. A more accurate assessment of the depth of the chlorophyll-*a* maximum was obtained from the CTD fluorescence profiles which revealed the chlorophyll-*a* maximum varied from as shallow as 5 m to as deep as 117 m between profiles. The cruise mean depth of the chlorophyll-*a* fluorescence maximum was 56.6 ± 26.1 m.

Integrated (0–150 m or 0 to deepest sampling depth) total chlorophyll-*a* concentrations ranged from 25.1 (station E1) to 69.9 (station B5) mg m^{-2} with an average of 48.0 ± 10.5 mg m^{-2} (Fig. 7). Stations located towards the centre of the Pemba Channel tended to exhibit lower integrated chlorophyll-*a* concentrations (Fig. 7). Stations located in the north east sector of the surveyed area (i.e. downstream of the upwelling and along the west coast of Pemba Island) had high integrated chlorophyll-*a* concentrations in excess of 55 mg m^{-2}. The shallow southwest stations exhibited low integrated chlorophyll-*a* concentrations.

Size-fractionated chlorophyll-*a* measurements consistently showed

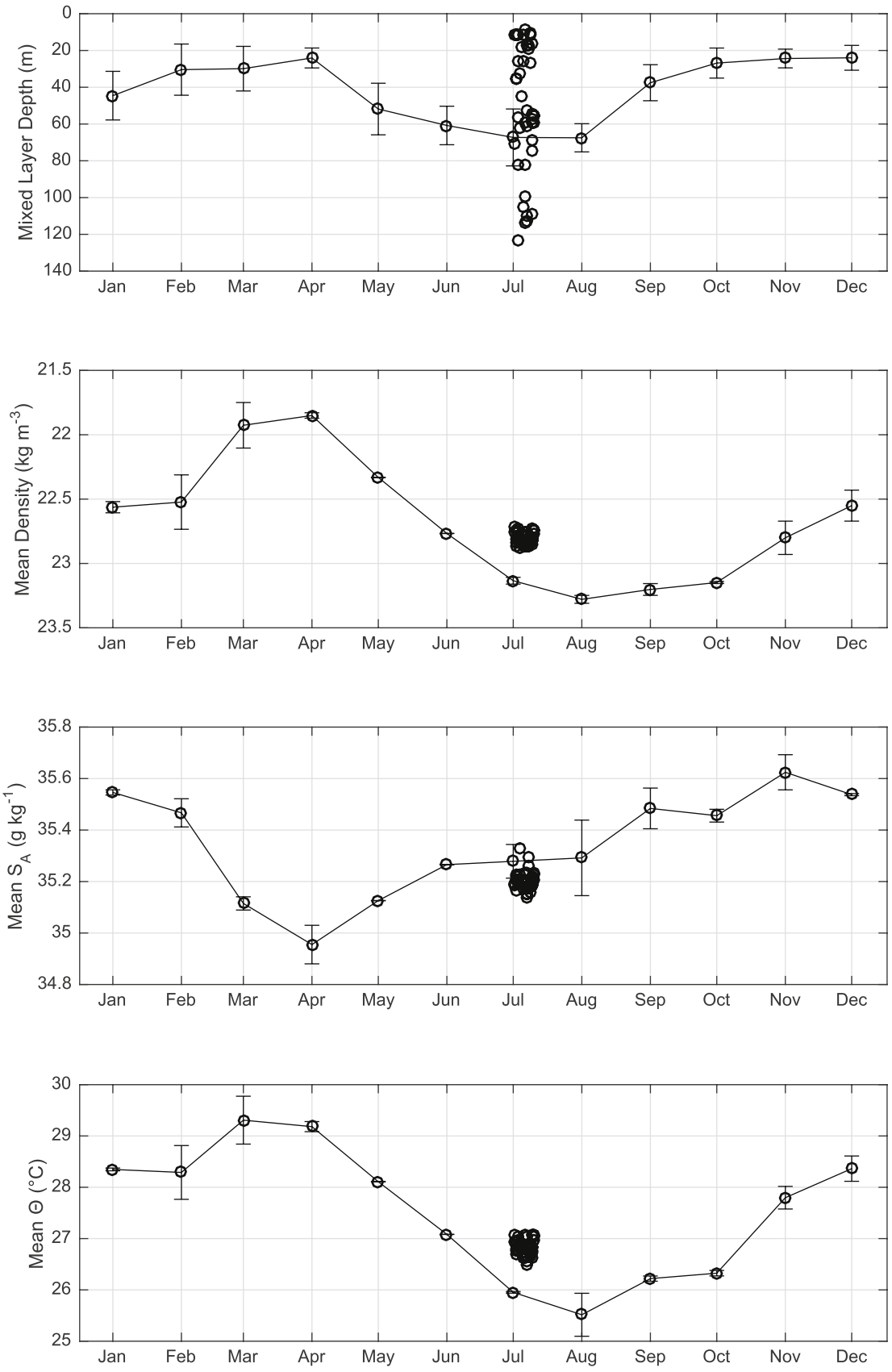

Fig. 4. Mean annual cycle of a) mixed layer depth, b) mean mixed layer density, c) mean mixed layer absolute salinity (S_A) and d) mean mixed layer conservative temperature (Θ) for Pemba Channel (black lines, monthly mean ± std) derived from the Argo based climatology of Holte et al. (2017). In-situ observations reported in this study are shown for comparison by open circles.

Table 1
Mean surface ocean and mixed layer conditions as observed in this study (June/July 2019)

Variable	Mean surface	Mean mixed layer
Conservative Temperature (C_T) (°C)	26.91 ± 0.18	26.82 ± 0.15
Absolute Salinity (S_A) (g kg^{-1})	35.200 ± 0.038	35.204 ± 0.035
Density (kg m^{-3})		22.806 ± 0.044
Total Chl-a (mg m^{-3})	0.39 ± 0.13	0.41 ± 0.10
Nitrate (μmol L^{-1})	0.09 ± 0.10	0.15 ± 0.16
Phosphate (μmol L^{-1})	0.12 ± 0.02	0.13 ± 0.02
Silicate (μmol L^{-1})	2.35 ± 0.33	2.38 ± 0.33
Mixed layer depth (m)	–	51 ± 35
Nitracline (1 μmol L^{-1}) depth (m)	–	90 ± 20
Nitracline gradient (μmol m^{-4})	–	169.70 ± 63.1

that the 0.7–2 μm size fraction, representing the picoplankton, dominated the total chlorophyll-*a* pool representing 80 ± 9% of the total chlorophyll-*a* pool in the upper 100 m (Table 3, Fig. 7). There was a notable reduction in the picoplankton contribution to ~50% at 150 m. Small nanoplankton (2–10 μm) typically represented ~12 ± 8% of the total chlorophyll-*a* pool in the upper 100 m with that contribution increasing to ~30% at 150 m. Larger nanoplankton (10–20 μm) and microplankton (>20 μm) size fractions contributed ~3 ± 4% and ~6 ± 3% on average to the total chlorophyll-*a* pool found within the upper 100 m. Typical contributions to the total chlorophyll-*a* pool may thus be summarised as 80% by picoplankton (<2 μm), 15% by nanoplankton (10–20 μm), and ~6% by microplankton (>20 μm).

Integrated chlorophyll-*a* concentrations for each size fraction ranged from 17.9 to 58.9 mg m^{-2} for the 0.7–2 μm picoplankton fraction, 0–10.8 mg m^{-2} for the 2–10 μm small nanoplankton fraction, 0.4–4.5 mg m^{-2} for the 10–20 μm large nanoplankton fraction, and 1–4.9 mg m^{-2} for the >20 μm microplankton fraction (Fig. 7). The spatial distribution of the picoplankton fraction followed the total integrated chlorophyll-*a* concentration with the highest values found in the north east of the channel. The small nanoplankton size phytoplankton concentration was high in the north of the channel and in the middle of the southern part of the channel whereas the large nanoplankton only showed a maximum concentration at station B5 and stations E3-E4. Finally, despite their low concentration, the microphytoplankton was most prevalent in the south west of the channel and rare in the middle of the channel.

3.7. Particulate concentrations and distributions

Particulate organic carbon and nitrogen concentrations at the surface ranged from 4.9 to 17.5 μmol C L^{-1} and 0.4–2.6 μmol N L^{-1} respectively (Fig. 5). Average particulate concentrations were 8.67 ± 3.01 μmol C L^{-1} and 0.86 ± 0.37 μmol N L^{-1}. Three prominent peaks in POC were visible in the data; immediately north of Zanzibar Island (~5.7°S), along the west coast of Pemba Island (~5.3–5.4°S) and close to the mainland shelf break in the north of the channel (~5°S). Corresponding peaks in PON were also apparent at these locations. The highest particulate concentrations of 14.5–17.5 μmol C L^{-1} and 1.1–1.6 μmol N L^{-1} were observed along the west coast of Pemba Island, but elevated concentrations >10 μmol C L^{-1} and >1.2 μmol N L^{-1} were also observed at shelf and shelf break stations to the north of Zanzibar Island.

Integrated pools of POC and PON only partially support the inference from the surface distribution of particulate pools for discrete regions of enhanced biomass (Fig. 9). Whilst integrated POC and PON were both elevated along the west coast of Pemba reaching concentrations of

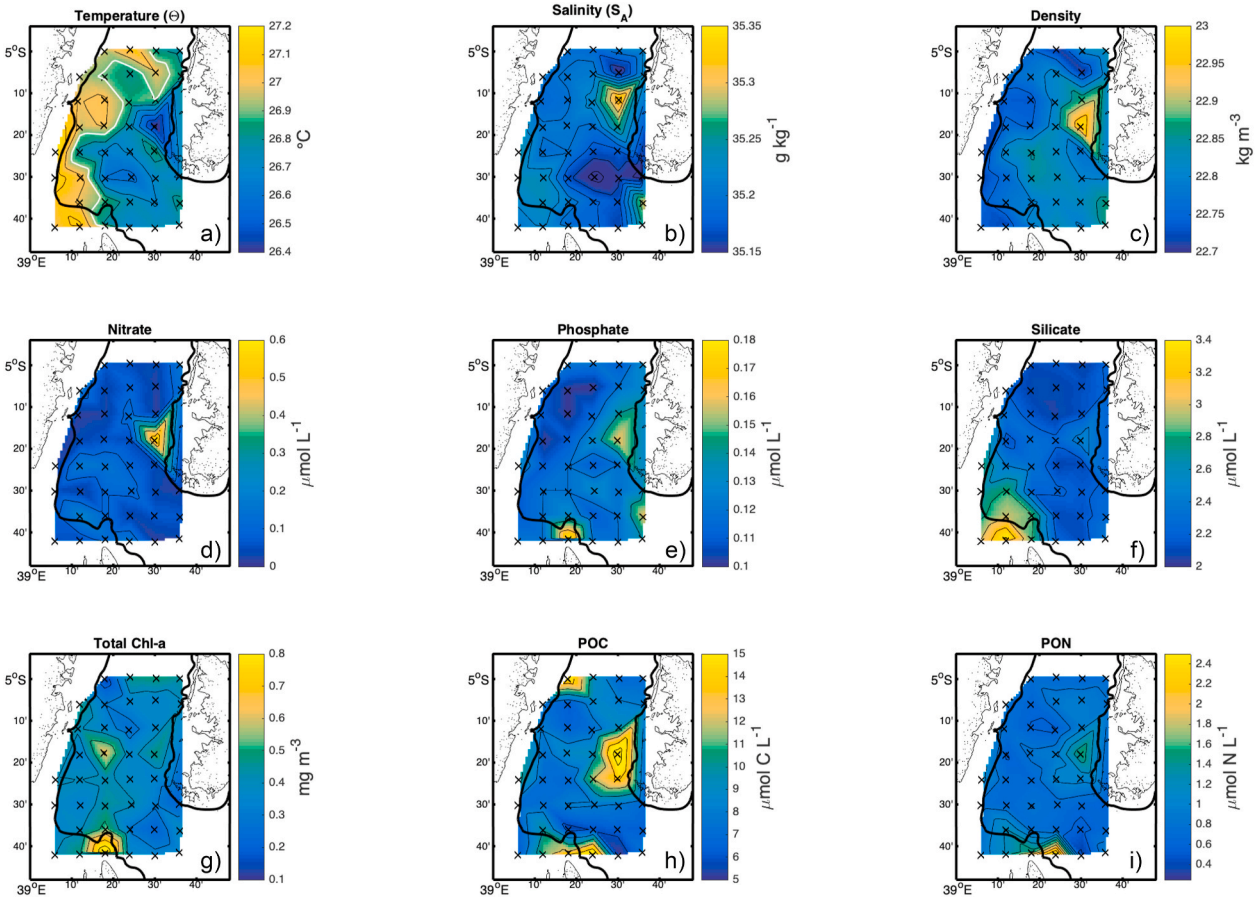

Fig. 5. Surface maps of a) Conservative Temperature, b) Absolute Salinity (S_A), c) density, d) nitrate, e) phosphate, f) silicate, g) total chlorophyll-*a*, h) particulate organic carbon (POC), i) particulate organic nitrogen (PON).

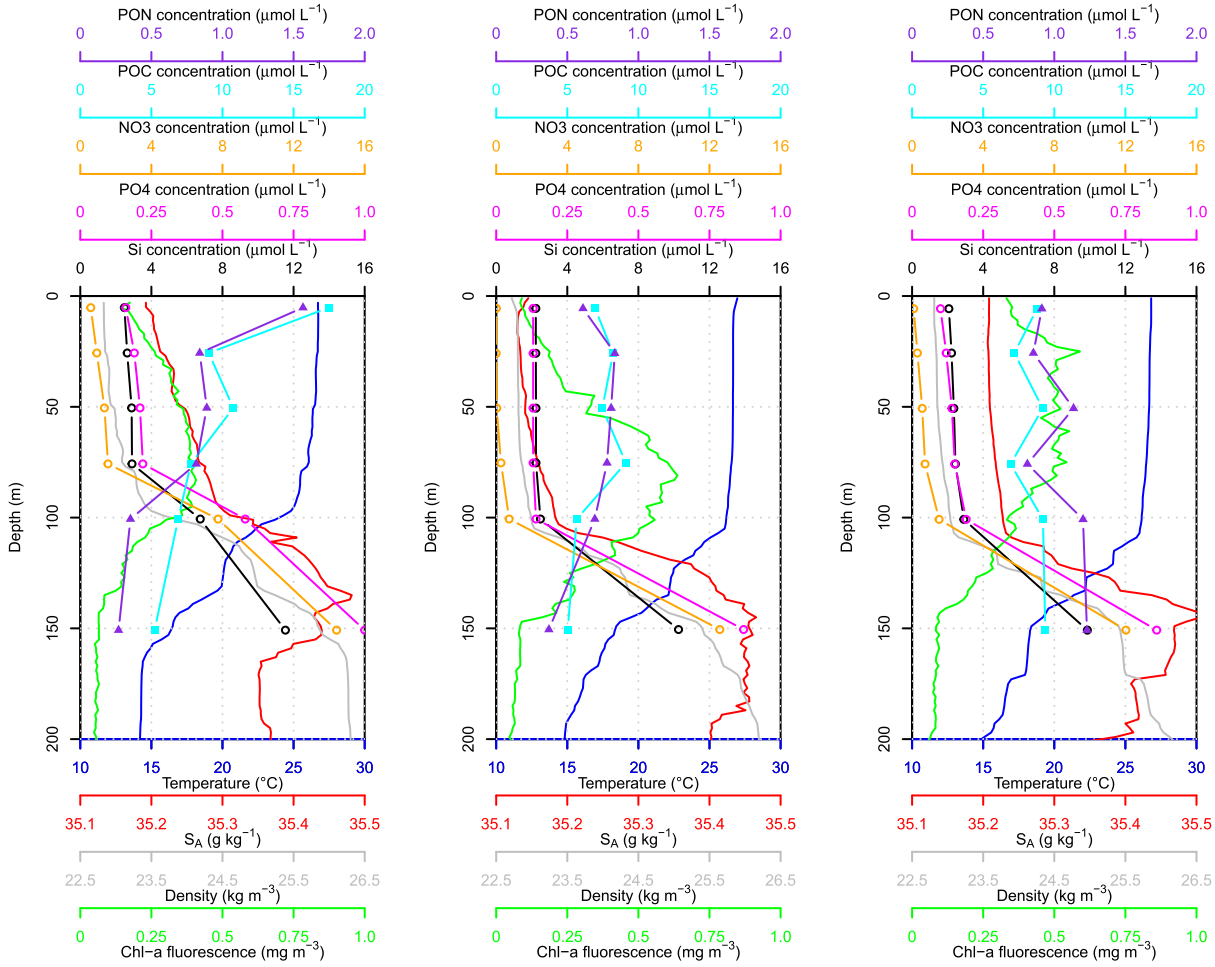

Fig. 6. Example plots showing the typical vertical distribution of selected parameters. Profiles shown relate to stations a) D4, b) G6, c) B3.

>1900 mmol C m^{-2} and >300 mmol N m^{-2} respectively, integrated pools were generally >1250 mmol C m^{-2} and >150 mmol N m^{-2} over much of the central and south eastern part of the channel. Integrated particulate pools were noticeably reduced towards the north and northwest stations (Fig. 9).

3.8. Particulate stoichiometry

The particulate C:N ratio ranged from 6.5 to 21.4 but on average the surface particulate pool was depleted in N relative to the Redfield ratio (C:N = 6.625) with a mean composition of 10.43 ± 2.48. Only at the inshore stations along transects G and H and close to the Zanzibar Channel did the POC:PON ratio fall below 8. The particulate pool was thus C rich/N poor relative to the Redfield ratio.

The integrated POC:PON ratio was much the same with an average of 10.33 ± 2.23 and a narrower overall range of 6.5–16.9 (Fig. 9). Comparable spatial patterns were evident and the lowest integrated POC:PON ratio was again observed close to northern entrance to the Zanzibar Channel.

3.9. Particulate isotope content

The isotopic content of particulate material found in surface waters revealed some intriguing spatial variability (Fig. 7). The $\delta^{13}C$ content ranged from −26.38 to −23.16‰ and exhibited a general north to south gradient with isotopically lighter material (>-24.5‰) found in the north of the studied area and a pronounced region of isotopically heavier material (<-24.5‰) in the southwest area near the shelf and Zanzibar Channel. The reason for this gradient is not clear but could reflect the influence of terrestrial inputs originating from the shelf areas, variation in sample detrital loadings or changes in the phytoplankton community. The $\delta^{15}N$ values meanwhile revealed a broadly homogenous particulate pool (mean 7.14 ± 1.58‰) with values ranging from 4.06 to 11.25‰ and no comparable north-south gradient (Fig. 7). However, a region of isotopically heavy material was present around the northern tip of Unguja Island with values > 8‰. There was also indication of a modest east-west gradient with the PON pool appearing to be isotopically lighter in the western half of the channel.

3.10. Coccolithophore abundances

A total of 38 coccolithophore species were identified (Appendix A). Total coccolithophore abundances were low ranging from zero at stations B2 and C4 up to 28,000 coccospheres L^{-1} at station H3 (Fig. 9). Species richness (S) varied from zero to 13 at individual stations, and the community diversity was generally low with Shannon-Wiener diversity indices (H′) of <2.5 (mean 1.34 ± 0.69). Pielou's eveness (J′) ranged widely from 0 at stations where single species were identified (stations C3, E2 and G1) to 0.969, where species were more evenly distributed (station D3). On average J′ was moderate to high (0.71 ± 0.27) and indicative of a system in which most species were equally abundant. Unusually low evenness values of <0.4 were observed at shelf stations F1 and H2.

Many species were present in low abundances and the spatial distributions were often patchy. *Gephyrocapsa oceanica* was the most widely distributed species, present at almost all stations, and with maximum

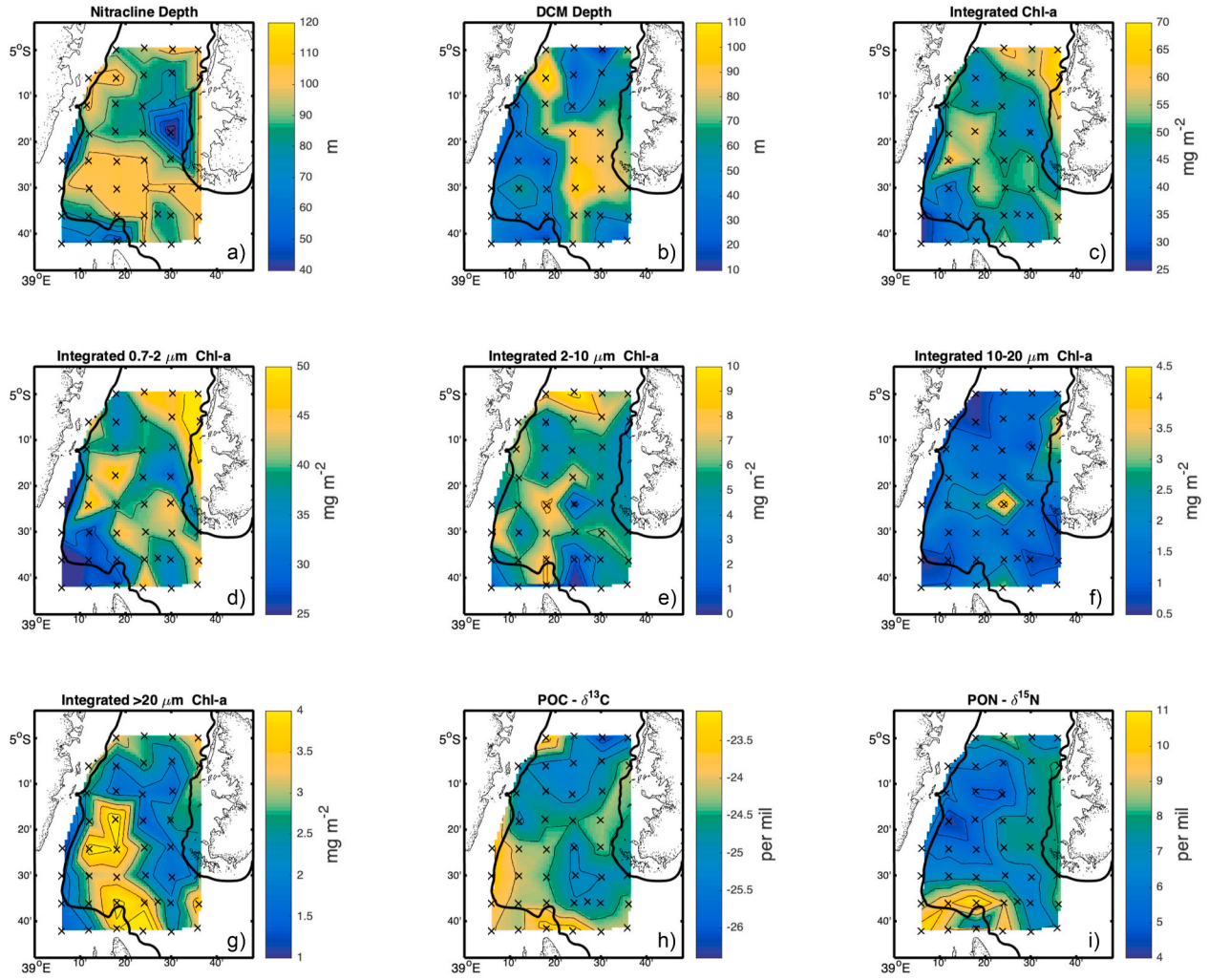

Fig. 7. Maps of a) nitracline depth (1 μmol NO_3^- L^{-1} contour), b) depth of deep chlorophyll maximum (DCM), c) integrated total chlorophyll-*a*, d) integrated picoplankton chlorophyll-*a* (0.7–2 μm), e) integrated small nanoplankton chlorophyll-*a* (2–10 μm), f) integrated large nanoplankton chlorophyll-*a* (10–20 μm), g) integrated microplankton chlorophyll-*a* (>20 μm), h) particulate $\delta^{13}C$ distribution, and i) particulate $\delta^{15}N$ distribution.

Table 2
Summary of integrated nutrient concentrations by transect. Nutrients were integrated using trapezoidal integration between 0 and 150 m or to the deepest possible sampling depth at each station. Mean transect values represent numeric averages of all stations along that transect.

Transect	Nominal Latitude (°S)	Integrated NO_3 (mmol m^{-2})	Integrated PO_4^{3-} (mmol m^{-2})	Integrated Si (mmol m^{-2})
A	5.00	311 ± 50	33 ± 4	513 ± 29
B	5.10	317 ± 83	36 ± 6	507 ± 50
C	5.20	434 ± 59	45 ± 6	581 ± 25
D	5.30	483 ± 195	47 ± 13	616 ± 124
E	5.40	249 ± 161	31 ± 15	446 ± 175
F	5.50	279 ± 99	33 ± 7	500 ± 70
G	5.60	286 ± 142	34 ± 12	483 ± 140
H	5.70	184 ± 195	24 ± 18	358 ± 194

abundances exceeding 20,000 coccospheres L^{-1} (Fig. 9). *G. oceanica* represented 48% of all observed coccolithophores in this study, though on a station-by-station basis *G. oceanica* could dominate or be absent from a sample (Fig. 10). Other species/genus with notable abundances were *Calciosolenia* spp. (maximum abundances of 5000 coccosphere L^{-1}), *Ophiaster* spp. (5000 coccosphere L^{-1}), and *Syracosphaera* spp. (over 6000 coccosphere L^{-1}). It should be noted that stations C3 and G1 give an unrealistic impression of dominance by single species/genus due to the very low coccolithophore abundances observed and these stations were otherwise devoid of coccolithophores. At stations truly devoid of coccolithophores (B2, C4) even loose coccoliths were in low abundance.

Rare species, with low contributions to total coccolithophore abundance and denoted as 'Others' in Fig. 10, collectively represented 8 ± 8% of the community assemblage but in some instances their contribution could collectively exceed 20%. Notable were stations B4, D4 and G4 where this category represented ~30% of the community. At these stations 8–10 species were identified including some unusual species. Station B3 contained the only specimen of *Rhabdosphaera clavigera* found and was one of only 3 stations where *Umbilicosphaera hulburtiana* was observed. Station D4 was notable for containing *Calcidiscus leptoporus* and *Florisphaera profunda* species which typically live in the mid to lower euphotic zone, particularly in this region (Stolz et al., 2015). Station G4 contained a modest increase in *Ophiaster* spp.

3.11. Community statistics

Bray-Curtis dissimilarities of log-transformed species abundance suggest intermediate dissimilarities between stations and up to five clusters of stations (Fig. 11). Whilst most stations were clustered together suggesting the presence of a largely homogenous community a small subset of stations from the southeastern entrance to the Pemba Channel and several stations from the northwest of the channel were

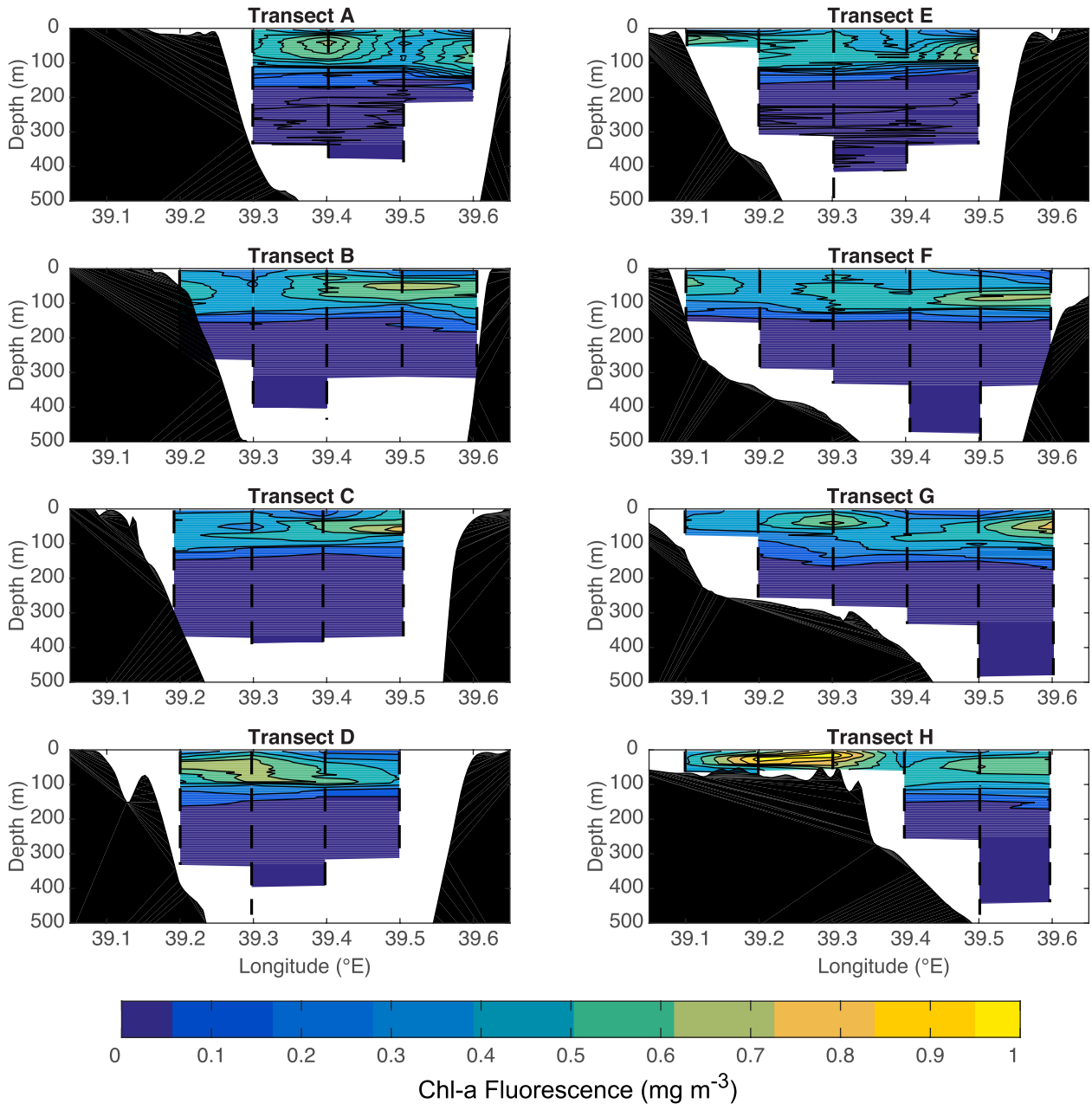

Fig. 8. Contoured cross sections of (calibrated) chlorophyll-*a* fluorescence presented by transect, see Fig. 1 for positions of each transect.

Table 3
Mean % contribution to total chlorophyll-*a* by size fraction over the upper 150 m of the water column.

Depth (m)	0.7–2 μm (% of total)	2 - 10 μm (% of total)	10 - 20 μm (% of total)	>20 μm (% of total)
5	80.7 ± 8	11.5 ± 6.1	2.9 ± 3.1	4.8 ± 2.5
25	83 ± 6.6	9.5 ± 5.8	3 ± 2.9	4.5 ± 1.8
50	78.9 ± 10.9	12.9 ± 8.4	2.6 ± 3	5.7 ± 3.3
75	78 ± 11.7	12.1 ± 9.4	3.3 ± 4.3	6.6 ± 3.8
100	77.4 ± 7.5	11.9 ± 7.7	3.9 ± 4.1	6.7 ± 2.4
150	51.2 ± 18.8	29.9 ± 20.6	8.1 ± 12.2	10.7 ± 5.7
Mean (0–100 m)	79.6 ± 8.9	11.6 ± 7.5	3.2 ± 3.5	5.7 ± 2.8

distinct. The results of the NMDS analysis broadly support the homogeneity of the coccolithophore community with few dissimilar stations (Fig. 11). In contrast the environmental data exhibited very low dissimilarities and 3 clusters of stations (Fig. 11). Notable was the distinction given to outlier stations D4 and H3, a clustering of the shallow southwesterly shelf stations, and a broad grouping of stations from the main channel, bisected by a cluster of stations along transects E and F. Vectors of environmental observations fitted to the NMDS ordination of coccolithophore count data revealed statistically significant ($p < 0.05$) relationships to temperature, silicate and turbidity whereas salinity, chlorophyll-*a*, NO_3 and PO_4 did not (Fig. 11).

3.12. Diatom community

Many small bicapitate *Nizschia* cells, approximately 10 μm long and 4 μm wide were observed throughout the SEM micrographs. These were most likely *Nitzschia bicapitata*, a cosmopolitan species in tropical and subtropical waters (Venrick, 1982, 1990, 1997; Lee and Fryxell, 1996; Fryxell, 2000). However, smaller bicapitate cells approximately 6 μm long and 2.5–3 μm wide were also observed and these may represent the

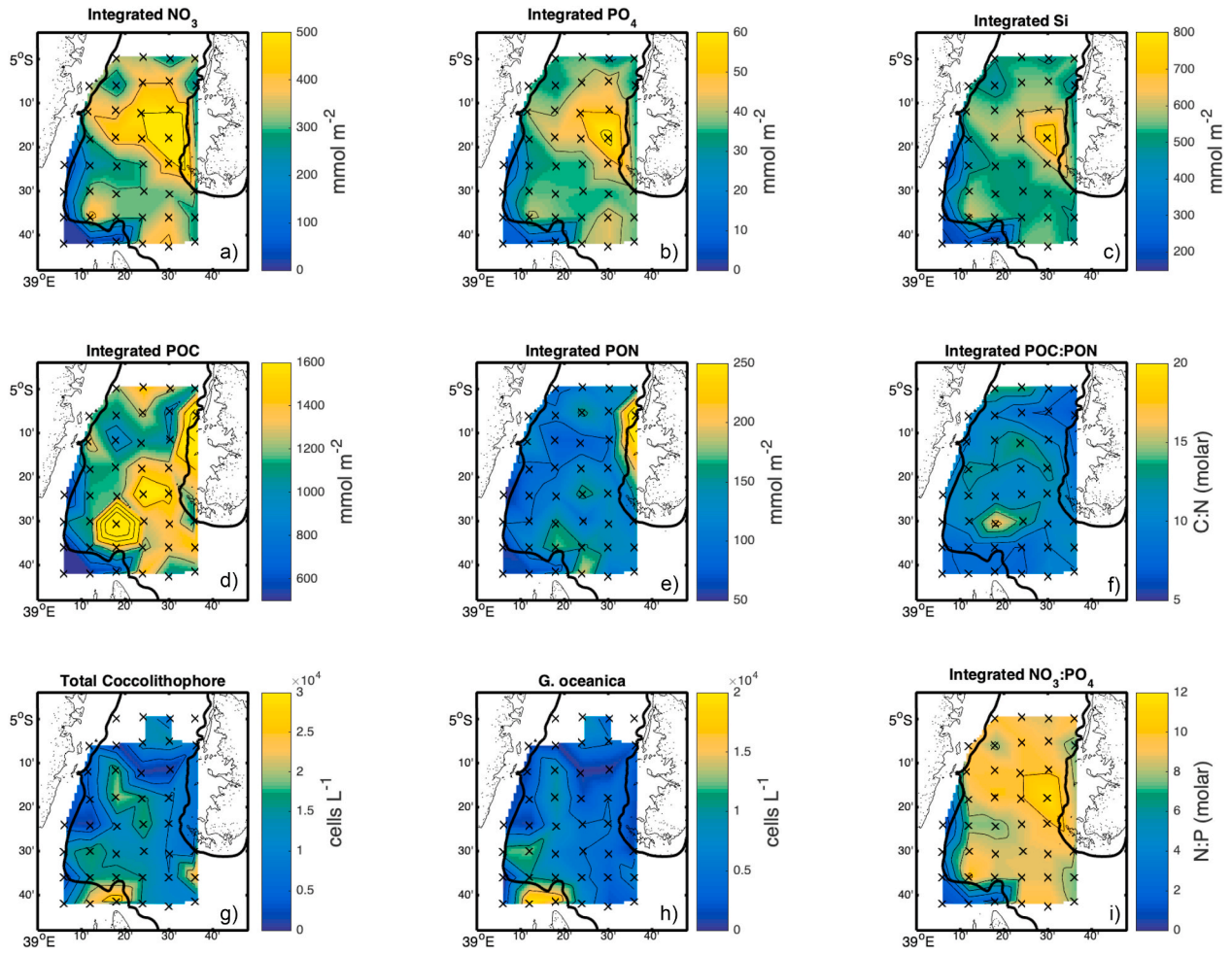

Fig. 9. Maps showing a) integrated NO_3^- pool, b) integrated PO_4^{3-} pool, c) integrated Si pool, d) integrated POC pool, e) integrated PON pool, f) integrated POC:PON ratio, g) surface distribution of total coccolithophore abundance, h) surface distribution of *Gephyrocapsa oceanica* and i) integrated NO_3^-:PO_4^{3-} ratio. Note that panels a–e have been scaled to emphasise spatial variability rather than the absolute range of concentrations described in the text.

species *Nitzschi leehyi* as described by Fryxell (2000). As identification of these smaller cells was uncertain, and as *N. leehyii* itself remains an uncertain classification (http://www.diatombase.org/aphia.php?p=taxdetails&id=657633#sources) such cells were counted as part of the large group of *Nitzschia* sp. observed. A brief summary of the diatom community as revealed by the SEM micrographs is presented in Table 4.

Chaetoceros species were rare and restricted to the southern half of the study site particularly the central stations along transects E to H (Fig. 12). The distribution of *Chaetoceros* cells was comparable, but not identical, to the distribution of the >20 μm chlorophyll-*a* fraction (Fig. 7). Though a qualitative distribution can only be described due to the small water volumes examined the appearance of *Chaetoceros* sp. along these southern transects may be indicative of advection into Pemba Channel from the south and southeast. The presence and distribution of *Chaetoceros* is noteworthy both as a potential food source for small pelagic fish (van der Lingen et al., 2009) and as a species that can be harmful to fish (usually farmed populations) when present in high abundance (Hansen et al., 2001; Fryxell and Hasle 2004; Hallegraeff 2004).

3.13. Zooplankton biovolume

Zooplankton settled volumes ranged from 0.169 to 0.760 mL m^{-3} and revealed a notable east-west gradient with higher mean settled volumes in the western half of the channel and a notable increase in the northern approaches to the Zanzibar Channel. There was no indication of elevated zooplankton biovolume in the vicinity of upwelling and only a very weak increase north (downstream) of the upwelling centre (Fig. 12). Integrated biovolume estimates however revealed a rather more complex picture (Fig. 12). In the vicinity of upwelling integrated biovolume estimates were low (<50 mL m^{-2}), whilst they were generally higher throughout the remainder of the Pemba Channel ranging up to 155 mL m^{-2}. A continuous band of high integrated biovolume (50–155 mL m^{-2}) was observed stretching from the southern entrance of the Pemba Channel, northwards along the mainland shelfbreak and into the northeastern waters of the channel. Highest integrated biovolumes (>100 mL m^{-2}) were observed in the western areas of the channel, whilst some enhancement could also be seen north of the upwelling.

3.14. Evidence of localised upwelling

The surface fields collectively provide evidence of upwelling at station D4 on the eastern side of the channel where elevated surface nitrate (0.5 μmol L^{-1}), reduced sea surface temperature (26.4 °C), elevated chlorophyll-*a* concentrations (0.48 mg m^{-3}) and elevated POC/PON concentrations (>10 μmol C L^{-1}/0.8 μmol N L^{-1}) were observed (Fig. 5). Interestingly and somewhat unexpectedly the strongest salinity anomaly (35.336 g kg^{-1}) was observed at station C4 to the north. Further examination of individual CTD profiles in this region revealed marked deviations from the mean in nitrate and salinity with elevated nitrate at station D4 extending from the surface to the nitracline. Examination of stations D3 to the west and C4 to the north revealed that a nitrate

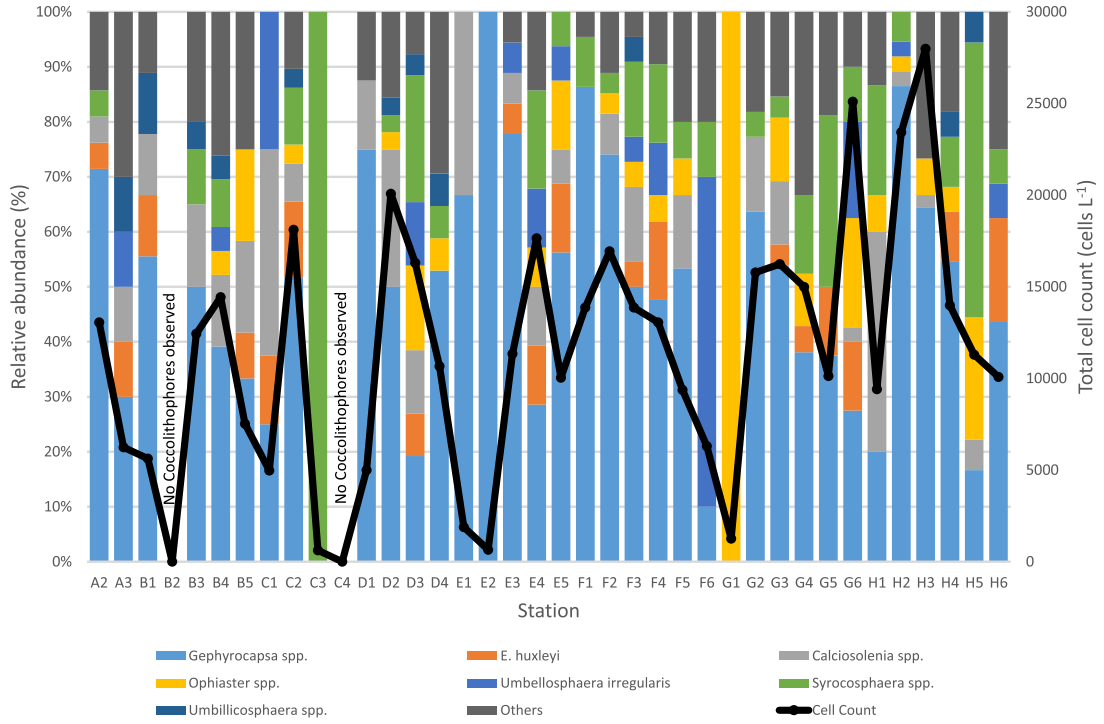

Fig. 10. Relative abundance plot of the coccolithophore community observed at sampled stations (columns) and total coccolithophore cell abundance at sampled stations (black line).

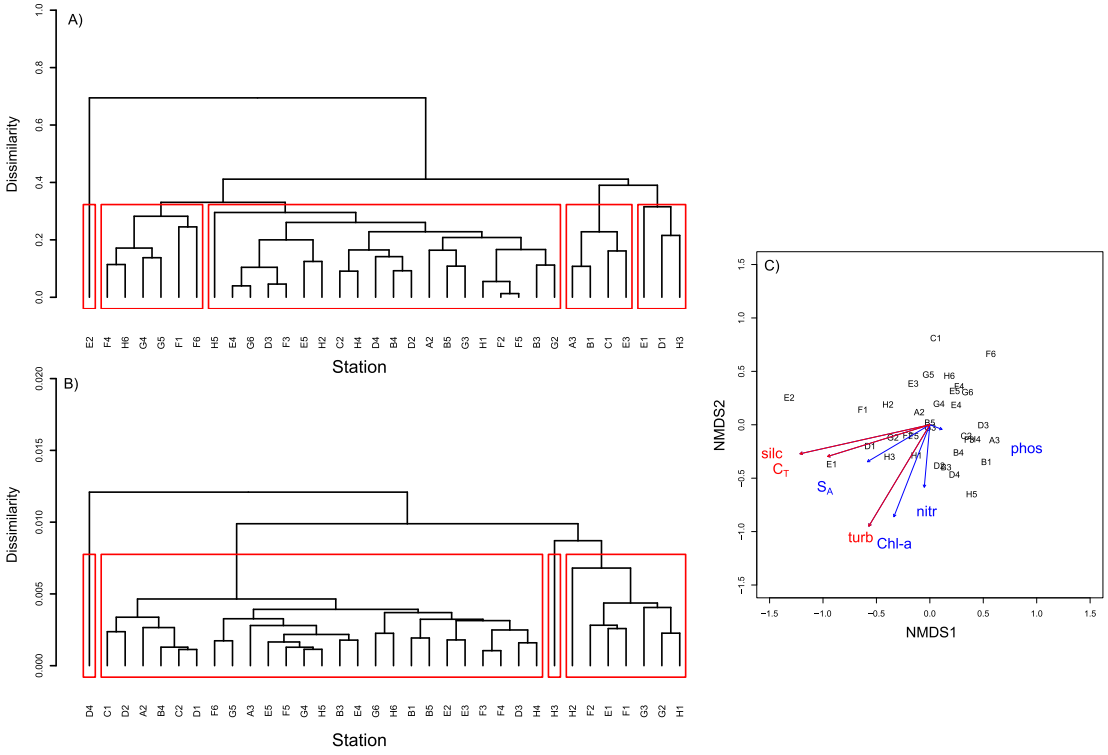

Fig. 11. a) Dendrogram of the average Bray-Curtis distance between sites based on log transformed coccolithophore count data, b) Bray-Curtis distance between sites based on environmental data (SST, SSS, turbidity, Chl-a, NO_3, PO_4, Si) and c) Non-Metric Dimensional Scaling (NMDS) of coccolithophore count data in relation to environmental data. Fitted environmental vectors shown in red are considered significant ($p < 0.05$). (For interpretation of the references to colour in this figure legend, the reader is referred to the Web version of this article.)

Table 4
Diatom genera or species observed in SEM samples of surface waters of Pemba Channel during the SE monsoon period.

Bacillariophyceae
Nitzschia spp.
Nitzschia bicapitata Cleve
Pseudo-nitzschia spp.
Chaetoceros spp.
Bacteriastrum spp.
Thalassiosira spp.
Thalassionema spp.
Rhizsosolenia spp.
Pleurosigma spp.
Leptocylindrus sp.
Navicula spp.
Mesoporus perforates
Tabularia spp.

concentration of 0.5 μmol L^{-1} was typical of waters found at ~80 m depth, comparable to the cruise mean depth of the 0.5 μmol L^{-1} isopleth of 81 ± 16 m, suggesting upwelling from at least this depth had occurred at station D4. Further examination of neighbouring salinity profiles found that stations D3 and D4 both had elevated salinities but it was station C4 that deviated most strongly with a surface salinity comparable to that observed at ~100 m on neighbouring profiles. The contoured cross-sections of salinity along transects C and D (Fig. 3) show upwelling of isohalines along these transects. A closer look at the TS diagram (Fig. 2) shows a curious kink at sigma 22.9 kg m^{-3}. The data points contributing to this feature represent profiles C4, D4 and G6, stations located along the western side of Pemba Island. Whilst elevated surface salinity at these stations likely indicates upwelling, particularly because of the depth of the observed anomalies, we cannot exclude the possibility that outflows from the narrow shelf around Pemba Island, particularly from Chake Bay are also involved.

4. Discussion

There are few previous studies from the Pemba Channel and a paucity of data more generally from this region. The World Ocean Database (v2013) contains only 18 hydrographic profiles either within or immediately adjacent to the Pemba Channel for the period 1909–1977 and nothing from more recent years. Notable contemporary work includes the African Coelacanth Ecosystem Programme (Scott 2004; Roberts et al., 2008; Barlow et al., 2011) which obtained ~20 CTD casts within the channel during fieldwork in 2004 and 2007, though this work is not yet fully published, and Stolz et al. (2015) who described the coccolithophore community within and around Pemba Channel. Older notable studies include Newell 1957, 1959, Harvey (1977) and Bryceson (1982)which remain influential.

The results reported here provide the first detailed assessment of environmental conditions within the Pemba Channel during the SE monsoon. Speculation around whether a limb of the EACC flows through the Pemba Channel or not was recently resolved by Semba et al. (2019) who used surface drifter data to confirm this. The new hydrographic observations reported here complement the findings of Semba et al. (2019) and show the presence of a strongly stratified surface layer, deep nutriclines and the widespread presence of SICW as a salinity maximum between 150 and 250 m depth throughout the channel. The results also

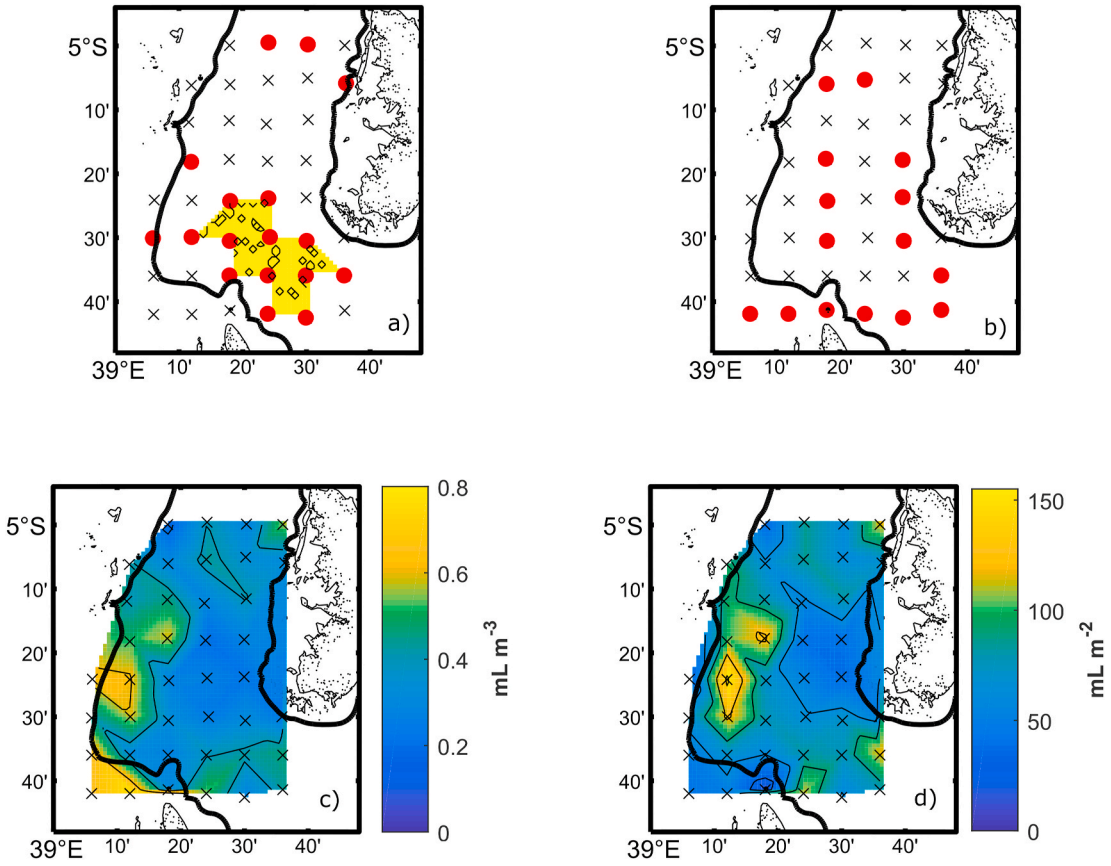

Fig. 12. Presence/absence maps of a) *Chaetoceros species and* b) *Pseudo-nitzschia* species from SEM micrograph analysis of surface (5 m) seawater samples. Black crosses indicate sampling points and absence of species, red circles indicate the presence of species, and where possible yellow shading is used to infer the main geographic extent of species distributions. c) 0–200 m mean zooplankton biovolume based on oblique hauls of 200 μm bongo nets, d) 0–200 m integrated zooplankton biovolume. (For interpretation of the references to colour in this figure legend, the reader is referred to the Web version of this article.)

reveal important spatial variability both vertically and horizontally that either has not been previously documented or has received only limited discussion (e.g. (Barlow et al., 2011).

Low nutrient conditions with severe N limitation characterised the upper surface waters of the Pemba Channel underpinned by deep nutriclines occasionally in excess of 100 m depth. Chlorophyll-*a* distributions revealed a subsurface maximum in the waters above the nitracline and on average this subsurface maximum was over 30 m shallower than the deeper nitracline. The strongly stratified conditions with low nutrient concentrations extending down to the nitracline argue against entrainment and significant nutrient supply to surface waters but the provisional estimate for the vertical diffusive flux of NO_3^- (163 ± 33 μmol NO_3^- m^{-2} d^{-1}) may be important for supporting the observed chlorophyll maximum - though this is dependent upon the nutritional requirements of resident phytoplankton. Given the dominance of the picoplankton size fraction in contributing to total chlorophyll-*a*, it is highly likely that species such as *Synechococcus* and *Prochlorococcus* and plankton groups such as the picoeukaryotes were present throughout the water column (e.g. Painter et al., 2014). It is also possible that the position and magnitude of the DCM was in large part driven by a reliance upon organic nutrient sources by *Prochlorococcus* as has been described elsewhere (Zubkov et al., 2003; Painter et al., 2008) or more generally

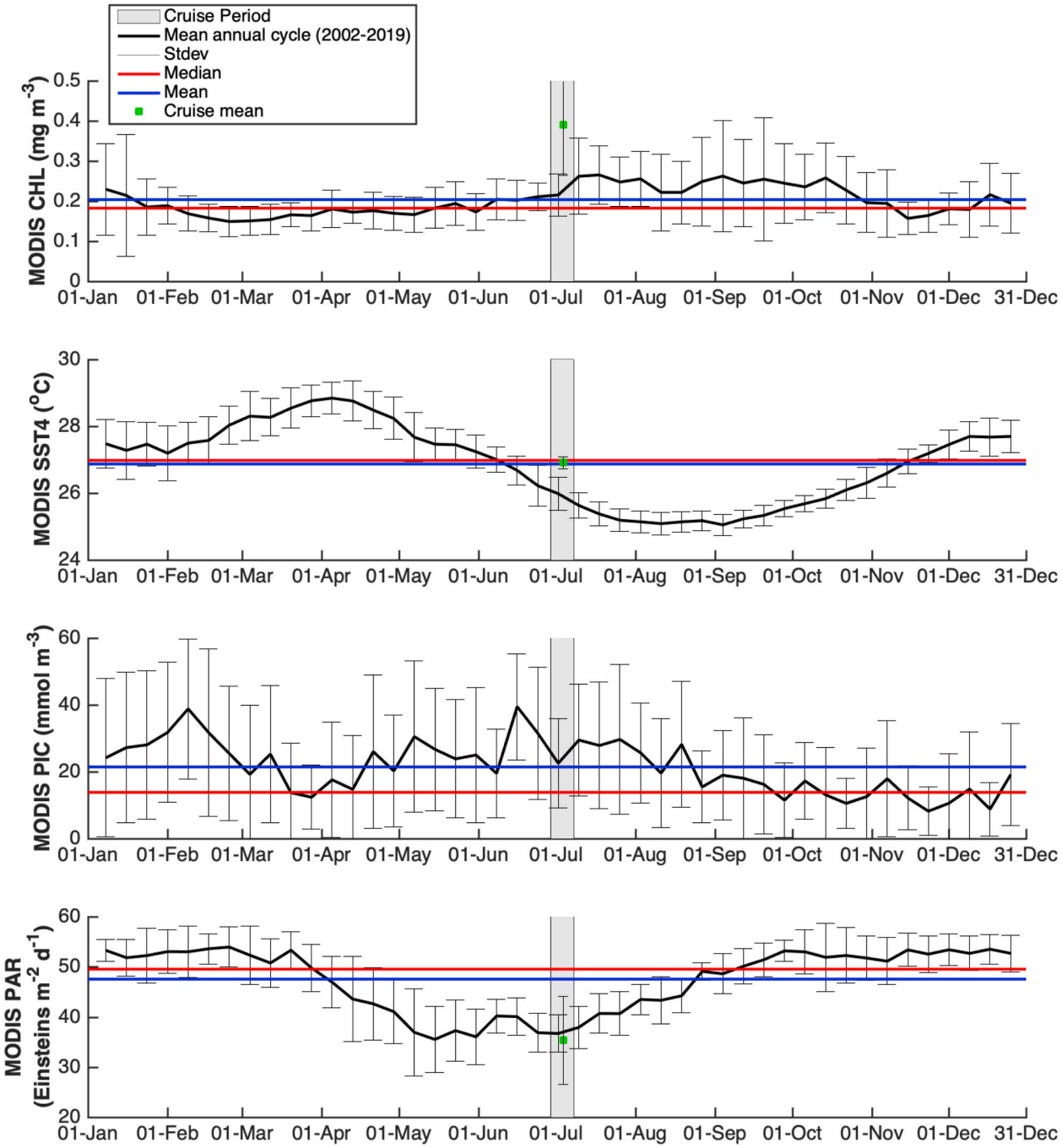

Fig. 13. Mean annual cycle of a) surface chlorophyll-*a* (CHL), b) sea surface temperature (SST4), c) particulate inorganic carbon (PIC), and d) photosynthetically active radiation (PAR) from the MODIS Aqua platform. Mean annual cycles were created from 8-day average datasets for the period 2002–2019 and for the geographic region 5–5.7°S, 39.3–39.6°E. Green squares (and errorbars) indicate cruise means ± std (where measured). (For interpretation of the references to colour in this figure legend, the reader is referred to the Web version of this article.)

on recycled N forms such as NH_4^+ (e.g. Mengesha et al., 1999) but without in-situ validation this remains a speculative conclusion.

Unlike traditional open ocean (sub)tropical settings where the DCM is usually located at depths equivalent to or below the 1% isolume, in Pemba Channel the vertical position of the DCM was found to vary significantly and over relatively short spatial scales (Fig. 8). On average the DCM was located around the 10% isolume but on individual casts could vary from as deep as the 0.3% isolume to as shallow as the 33% isolume. This variability is suggestive of a dynamic rather than quiescent environment. The characteristic DCM of subtropical waters, where a thin but pronounced chlorophyll maxima is found at the base of the euphotic zone, was occasionally observed notably at stations C4, D3, E4, F4, F5, F6 located in the central and eastern half of the channel but was otherwise not representative of vertical chlorophyll-*a* distributions for the remaining stations. This grouping of stations, and the prevailing circulation and northwards flow of the EACC suggests that the characteristic tropical DCM was progressively lost or masked due to vertical mixing, increased phytoplankton growth in surface waters or proximity to the narrow shelf along the mainland.

4.1. Seasonality

Though the time limited observations reported here preclude adequate discussion of biological seasonality within the channel it is evident from remote sensing observations (Fig. 13; see also Painter 2020) that peak annual surface chlorophyll-*a* concentrations occur over the central and deeper waters of Pemba Channel during the SE monsoon (Jun–Oct), a period when sea surface temperatures also decrease (Fig. 13). This is coincident with a deeper mixed layer (Fig. 4) which conventionally may indicate entrainment of deeper nutrient waters and enhancement of primary production (e.g. Hartnoll (1974)). The nutrient data presented here do not show high surface nutrient concentrations throughout the channel thus the assumption of entrainment following deepening of the mixed layer is likely invalid. In support of this most individual mixed layer depth estimates and the average for the cruise (51 m) were shallower than respective nitracline depths (mean depth 90 m) though the timing of the in-situ observations preceded the timing of the annual SST minima by about 6 weeks and further cooling and mixing likely occurred. Mean annual surface particulate inorganic carbon (PIC) concentrations, often used to indicate the seasonal phenology of coccolithophores (Hopkins et al., 2015), appear highly variable within the channel (Fig. 13) but suggest that the cruise occurred during the annual PIC maximum (May–Aug), which may be considered synonymous with peak coccolithophore abundance. This then implies that the low coccolithophore cell counts reported here for the SE monsoon period likely reflect typical conditions. Surface PAR measurements meanwhile place the cruise just after the annual minimum (Fig. 13). Whilst the seasonal timing of peak chlorophyll-*a* within the channel agrees with the annual cycle of productivity for the Western Indian Ocean (Cushing 1973), this is at odds with the timing of peak chlorophyll-*a* for the Zanzibar Channel which reportedly occurs during the NE monsoon (Bryceson, 1982; McClanahan 1988). The deeper Pemba Channel is thus more similar to the wider WIO region than to the neighbouring Zanzibar Channel.

4.2. Phytoplankton

Phytoplankton species diversity in Tanzanian coastal waters, like many tropical regions, is considered to be high with reports of ~200–275 individual taxa present (Bryceson, 1977; Lugomela, 1996; Lugomela and Semesi, 1996; Mgaya, 2000; Lyimo, 2011). Spatiotemporal variability in species distributions and abundance along the Tanzanian coast or more widely long the East African coastline is not well described in the literature (Huggett and Kyewalyanga, 2017), but given the prevailing tropical conditions and low nutrient availability the phytoplankton community should be skewed towards the picoplankton (0.2–2 μm) size fraction. Confirmation of this is generally lacking but in Kenyan coastal waters Kromkamp et al. (1997) reported 40–60% of total chlorophyll-*a* in the picoplankton size fraction (<3 μm) whilst Ranaivoson and Magazzu (1996) found a comparable 34–66% in waters off Madagascar. The present study finds that picoplankton (0.7–2 μm) represent an average of 80% of available chlorophyll-*a* throughout the upper 100 m of the water column with this contribution decreasing sharply at the base of the euphotic zone (1% isolume). To date, most phytoplankton studies from this region have focused on the larger nano- and microplankton whereas it is the smaller picoplankton that likely drive spatial and temporal variability in chlorophyll-*a* patterns. Thus, efforts to use remotely sensed chlorophyll-*a* distributions to understand the productivity of these waters would benefit from greater consideration of the ecological role and trophic status of picoplankton, particularly if attempts to link surface Chl-a to other sectors such as fisheries are made. In particular, planktivorous fish, such as the regionally important small pelagic species (Sekadende et al., 2020) typically target larger phytoplankton or zooplankton (e.g. van der Lingen et al., 2009).

Observations of the coccolithophore community, both in terms of identified taxa and cellular abundances, were highly comparable to the only other known study from these waters. Stolz et al. (2015) reported 47 coccolithophore species in and around Pemba Channel with abundances that ranged from zero to 23,000 coccospheres L^{-1}. The similarity suggests a degree of temporal and possibly regional stability in both the community composition and in typical abundances.

The results of the multivariate analyses generally indicated low levels of dissimilarity between stations in the coccolithophore community. This may be due to the relatively low water volumes sampled and in particular to the low abundances of many species but as the community was in general comparable to the previous assessment by Stolz et al. (2015), low levels of dissimilarity likely indicate small scale heterogeneity and patchy distributions rather than genuine geographic variability. More intriguingly, there appeared to be significant relationships to temperature and silicate. A notable thermal gradient was identified across the channel (Fig. 5) which seems to be a major factor in structuring the coccolithophore community and perhaps even influencing overall surface abundances (Fig. 9). The link to silicate is less clear. Some coccolithophore species are now known to have a biological requirement for silicate yet *G. oceanica*, which was widespread throughout the Pemba Channel, does not have this requirement (Durak et al., 2016). *G. oceanica* is however known to exhibit a strong relationship to higher silicate concentrations and has found use as a proxy species for mild upwelling and as an indicator of productive periods (Narciso et al., 2016).

Observations of the coccolithophore community and of larger potentially harmful bloom forming diatoms do suggest an important role for larger nano- (2–20 μm) and microplankton (>20 μm) size fractions in these tropical coastal waters. Gradients in the plankton community from shallow to deep waters are known (Wickstead, 1962, 1963) but likley require re-evaluation in light of the improved understanding of the regional oceanography. In this study the >20 μm chlorophyll-*a* fraction was predominantley located north (downstream) of Unguja Island and may have been advected away from the shelf areas, including the Zanzibar Channel, which are known to host larger nano- and micro-phytoplankton (Moto et al., 2018), whilst mid-channel waters otherwise hosted smaller picoplankton advected into the channel from the Indian Ocean by the EACC.

The patchy distribution of *Chaetoceros* sp. and its comparable positioning to the region of high >20 μm chlorophyll-*a* tends to support a conclusion from Barlow et al. (2011) that there are patterns of spatial variability in the phytoplankton community structure within Pemba Channel that are poorly understood or measured. The SEM micrographs examined here, though not suited to a complete assessment of larger phytoplankton, do tend to show greater diatom diversity at the inshore stations of Transect H, particularly station H3, suggesting that there are important spatial gradients present within shallow sheltered waters. Nevertheless, unlike the study by Barlow et al. (2011) the

size-fractionated chlorophyll-*a* results reported here revealed a persistent dominance by the picoplankton size-fraction at all stations.

4.3. Zooplankton

The distribution of zooplankton biovolume was comparable to the temperature gradient across the channel (Fig. 5) most likely highlighting the influence of the shelf which is usually enriched in zooplankton with shallower water depths also having a concentrating effect. The integrated biovolume (Fig. 12), which removes the influence of a shallower water depth, showed some resemblance to the distribution of the >20 μm chlorophyll-*a* fraction in that both were elevated in the western sector of the channel. It is well established now that most herbivorous copepods feed efficiently on larger (>20 μm) phytoplankton cells, most likely diatoms, which could explain this localised increase in zooplankton biovolume. However, total chlorophyll-*a* is rarely correlated to zooplankton abundance in oligotrophic areas mostly due to differing time responses by these two trophic compartments. The comparable distribution may also be due to the fact that biovolume measurements typically underestimate the more abundant small zooplankton organisms which feed on smaller phytoplankton and microzooplankton and are thus not well represented by the total biovolume. Influence from the Pangani River, which is otherwise minimal for all other variable distributions, may also play a role though this is far from clear. The biovolume measurements are within the range of other studies conducted in the south west Indian Ocean (Huggett, 2014; Noyon et al., 2019). Zooplankton biovolume in the western and central Pemba Channel would appear typical of biovolume content within waters of the EACC advected into the channel. Upwelling along Pemba Island appears to have limited impact on zooplankton biovolume at the exact station of the upwelling (i.e. D4) but higher (integrated) biovolumes to the north may be associated with the northwards advection of zooplankton, though this is however speculation. Considering the strong current in the area and that zooplankton need about 10–15 days to respond to an increase in food availability (Hoover et al., 2006) it is unlikely that zooplankton would have enough time to grow and reproduce in response to that upwelling unless a retention mechanism was also present, thus upwelling along Pemba Island appears to have limited and possibly even no impact on zooplankton biovolume within the channel.

4.4. Upwelling

Evidence for upwelling along the tropical East African coast remains equivocal (Bakun et al., 1998), and the more tangible impacts of upwelling such as elevated nutrient and chlorophyll-*a* concentration, decreased surface temperatures and altered nutrient stoichiometries remain unreported (but see Jebri et al., 2020). In this study upwelling from at least 80–100 m depth was identified along western Pemba Island in a region where there is steep bathymetry and strong current flow (Fig. 1; Fig. 5). This upwelling appears spatially limited to a region $\ll$10 km^2 (based on the horizontal CTD spacing) and is of unknown temporal duration. The presence of deep living coccolithophore species in the surface waters of station D4 is consistent with the hydrographic and nutrient datasets that suggest a strong, though spatially localised upwelling. According to the vertical distributions of the coccolithophores *C. leptoporus* and *F. profunda* reported by Stolz et al. (2015) for Pemba Channel the abundance maxima for these species are usually found at depths of between 75 and 100 m. This depth interval is consistent with the source depth for water with a nitrate concentration of 0.5 μmol L^{-1} as measured at the surface at station D4. Meanwhile the widespread presence of *G. oceanica* can also be interpreted as being consistent with prolonged periods of (mild) upwelling (Narciso et al., 2016).

Surface POC and PON concentrations at station D4 were elevated compared to most other stations and relative to the cruise mean surface POC concentrations were over 2-fold higher (17.47 vs 8.67 ± 3.01 μmol C L^{-1}) whilst PON concentrations were 1.8-fold higher (1.6 vs 0.86 ± 0.37 μmol N L^{-1}). This is suggestive of a productivity response to the increased surface NO_3 concentrations. However, despite integrated nutrient pools largely supporting the centre of upwelling at and around station D4 the integrated particulate pools do not show a corresponding increase (Fig. 9). Integrated POC at station D4 was only 12% higher than the cruise mean and integrated PON was actually ~10% lower than the cruise mean. In fact, the integrated POC concentration at station D4 was only the 12th highest observed throughout the cruise, whilst integrated PON was the 22nd highest.

The spatial variability in the particulate isotopic content also suggests complex origins underlying the POC and PON pools (Fig. 7). Phytoplankton $\delta^{13}C$ and $\delta^{15}N$ values do vary widely (Rau et al., 1982; Montoya, 2008) but the observed $\delta^{13}C$ (~-26.4 to −23.2‰) and $\delta^{15}N$ (~4.1–11.3‰) values are within natural limits. Nevertheless, the observed spatial gradients likely indicate important underlying processes but the data are insufficient to reach definitive conclusions. A terrestrial influence on the $\delta^{13}C$ values recorded within surface POC from shallow shelf stations is feasible but persistent terrestrial inputs are unlikely as they would also be associated with increased turbidity which would, over time, negatively impact known coral reef distributions UNEP-WCMC, 2018. Interestingly, the $\delta^{13}C$ distribution may actually result from shifts in the phytoplankton community, particularly the relative contribution of diatoms, with different phytoplankton groups known to exhibit different $\delta^{13}C$ values (Hansman and Sessions 2016). The $\delta^{15}N$ signature may reflect the degree of oligotrophy whereby more oligotrophic waters are more depleted in $\delta^{15}N$ compared to newly upwelled nitrate (Saino and Hattori 1980). Hence the higher $\delta^{15}N$ signature coming from the Zanzibar Channel, on the northern tip of Ungunja and on the eastern side of the Pemba Channel may indicate new nutrient input into the system, while the more $\delta^{15}N$ depleted observed in the middle of the Channel may represent the highly oligotrophic EACC. This may highlight some physical processes of upwelling as discussed here as well as the influence of the shallow Zanzibar Channel, but it also suggests the possibility of some small scale retention features. Further work is required to confirm these hypothesises.

The integrated NO_3 pool at station D4 was almost 2.5-fold higher than the cruise mean (756 vs 306 mmol N m^{-2}). For silicate and phosphate the relative increase was smaller at 1.6 and 1.9-fold respectively. Based on assumptions regarding the timescale over which upwelling could maintain an excess NO_3 concentration (150 days i.e. SE monsoon period June to October), the magnitude of the excess relative to the regional mean (i.e. 450 mmol N m^{-2}), and the Redfield ratio for organic matter synthesis, an excess primary production rate of 0.24 g C m^{-2} d^{-1} may be calculated. But how does this compare to in-situ productivity rates?

Primary production measurements within the central waters of Pemba Channel are rare (Painter 2020). Barlow et al. (2011) measured productivity rates of 1.08–1.34 g C m^{-2} d^{-1} at three stations in the channel, and away from the epicentre of upwelling, during the late SE monsoon period (October). Cushing (1973) estimated a comparable mean productivity of 1.2 g C m^{-2} d^{-1} for coastal East Africa (0–10°S) during the SE monsoon period whilst the annual mean productivity for the Somali Coastal Current Large Marine Ecosystem, which encapsulates the Pemba Channel, is estimated to be 0.76 g C m^{-2} d^{-1} (GEF/TWAP, 2015). Barlow et al. (2011) report the highest productivity rates so far recorded for this region () thus the estimate of production supported by upwelling calculated here (0.24 g C m^{-2} d^{-1}) would equate to ~18–22% of the productivity rates reported by Barlow et al. (2011). Thus, upwelling could locally enhance primary production along the western edge of Pemba Island by ~20% relative to typical conditions elsewhere within the channel. This estimation is however associated with high uncertainty and direct confirmation of enhanced productivity rates is required particularly given the limited role NO_3^- and new production is assumed to play in regional productivity (Mengesha et al., 1999).

4.5. Implications for the management of the marine environment and living marine resources

4.5.1. Upwelling, biological productivity and fisheries

The identification of a discrete upwelling signature along the west coast of Pemba Island and the potential enhancement of typical productivity rates by ~20% requires further investigation as the waters impacted by this upwelling exhibited a mixed biological response. Enhanced biological productivity, as evidenced by increased surface POC and chlorophyll-*a* concentrations (Fig. 5) suggests a direct response to higher nutrient concentrations yet integrated POC and chlorophyll-*a* pools were not remarkable compared to other stations or to the cruise means. This contradiction may relate to the strength of upwelling and the physical movement of water with the upwelling sufficiently strong enough to create observable disturbances at the sea surface (personal observations). It is probable therefore that there is little or no opportunity for biomass to accumulate deep in the water column as it is continuously advected vertically by upwelling and concentrated near the sea surface before being rapidly advected horizontally by the prevailing current. Integrated chlorophyll-*a* concentrations do increase immediately downstream of the upwelling and to the north of the studied area (Fig. 7), suggesting, perhaps, a delayed response and horizontally offset productivity region.

Regardless of such apparent spatial contradictions any enhancement of productivity rates due to upwelling is likely to be of wider significance, particularly for local fisheries and the impacts may manifest in one or several ways. Localised areas of enhanced (phytoplankton) productivity may ultimately lead to aggregations of fish or act as important feeding grounds particularly for small pelagic fish which are planktivorous (feeding on larger phytoplankton but mainly zooplankton). Persistent upwelling leading to increased particulate biomass at the surface in one or more localities may also be of significance providing a regular source of food for some fish species against a background of otherwise low particulate concentrations. Tellingly, the upwelling feature identified here is in the same geographic position as previously shown as hosting high concentrations of small pelagic fish (Iversen et al., 1984). Key unknowns remain however including the spatiotemporal duration of upwelling, the underlying physical mechanism, whether the upwelling experiences any seasonality and what, if any, are the impacts on higher trophic levels particularly zooplankton. Anecdotal observations of surface boils, including visual observations made during the cruise, suggest that upwelling is likely linked to the dynamics of a fast-flowing current encountering steep bathymetry rather than to wind induced coastal upwelling (Jebri et al., 2020). The northward velocity of the EACC peaks at ~1.7 m s^{-1} during the SE Monsoon period (Semba et al., 2019) thus any bathymetric obstacles to the current are likely to induce considerable vertical disturbances. As the EACC slows by ~24% to ~1.3 m s^{-1} during the NE monsoon (Semba et al., 2019) any reduction in velocity is likely to impact upwelling intensity but may not necessarily cause a cessation of that upwelling. Better understanding of the mechanism driving this localised upwelling is essential for better management of fisheries resources and local knowledge from the fishing community may be an important and valuable source of information in helping to clarify links between surface signatures of upwelling and distributions of small pelagic fish.

4.5.2. Anthropogenic nutrient impacts

The surface waters of Pemba Channel appear N limited as indicated by very low NO_3^-:PO_4^{3-} ratios (<0.7) and this may be linked to (though not caused by) high N_2 fixation rates reported from these waters (Lugomela et al., 2002). Even when considering the impact of upwelling on nutrient concentrations the upper ocean remains NO_3^- poor relative to PO_4^{3-} (Fig. 9). NO_3^- is not the only N source for phytoplankton productivity however and regionally upper ocean productivity has been shown to be highly reliant upon regenerated N sources such as NH_4^+ (Mengesha et al., 1999). Nevertheless, low N:P conditions suggest that these waters may be susceptible to anthropogenic N inputs which in turn could lead to the occurrence of nuisance or harmful algal blooms. Across the region, there is a long established practice of discharging municipal and industrial effluents directly to the sea (UNEP 2015). Such inputs could conceivably be linked to increased occurrences of harmful algal bloom species, yet whilst the occurrence of HAB species is regionally monitored (Hansen et al., 2001), regular monitoring for such species around the Zanzibar archipelago is currently lacking (Kyewalyanga and Lugomela 2001).

5. Conclusions

A comprehensive dataset of oceanographic and biogeochemical observations collected within Pemba Channel during the SE monsoon period has been presented. The dataset reveals.

- A clear dominance of the chlorophyll-*a* pool by picoplankton (<2 μm) which represent 80% of total chlorophyll-*a*.
- Localised upwelling along the western edge of Pemba Island with corresponding and spatially localised (~10 km^2) chemical and biological impacts. Salinity and nutrient fields suggest upwelling from 80 to 100 m depth. Noteworthy, was the occurrence of deep living coccolithophore species from 75 to 100 m depth at the sea surface in the centre of the upwelling feature.
- Despite ~2-fold increases in integrated concentrations of NO_3 and PO_4 in the upwelling region and approximately 2-fold increases in surface POC and PON concentrations there was no depth integrated increase in POC or PON in the immediate vicinity of upwelling. Nevertheless, a notable east-west gradient in integrated chlorophyll-*a* and POC pools suggests greater productivity in the eastern Pemba Channel, consistent with the region and impacts of upwelling.
- Upwelling is tentatively estimated to enhance local productivity rates by 20% relative to typical background rates but this estimate is associated with high uncertainty and in-situ confirmation is suggested as a high priority objective for future research.
- Despite the presence of upwelling the surface waters of Pemba Channel remain naturally depleted in NO_3^- relative to PO_4^{3-} leading to low N:P conditions. The widespread occurrence of N limitation (or residual P) may therefore increase the risk of deleterious effects related to anthropogenic N inputs.

Declaration of competing interest

The authors declare that they have no known competing financial interests or personal relationships that could have appeared to influence the work reported in this paper.

Acknowledgements

This work contributes to the Sustainable Oceans, Livelihoods and food Security Through Increased Capacity in Ecosystem research in the Western Indian Ocean (SOLSTICE-WIO) programme (www.solstice-wio.org) , a four-year collaborative project funded through the UK Global Challenges Research Fund (GCRF) under NERC grant NE/P021050/1. We are grateful to Dr. Jean Harris and Wild Oceans (http://wildtrust.co.za/wildoceans/) for being willing to bring the M.Y. *Angra Pequena* into Tanzanian waters and we thank the Master and crew for their excellent assistance and consistent good humour throughout the cruise. We also thank Kristian Seterås at the Norwegian Institute of Marine Research for sourcing reference materials.

Appendix A. Identified Coccolithophore Species and grouping for multivariate analyses

Species	Group
Acanthoica quattrospina	*Other*
Algirosphaera robusta	*Other*
Alisphaera sp.	*Other*
Calcidiscus leptoporus	*Other*
Calciopappus rigidus	*Other*
Calciosolenia brasiliensis	*Calciosolenia* spp.
Calciosolenia murrayi	*Calciosolenia* spp.
Coronosphaera mediterranea	*Other*
Cyrtosphaera sp	*Other*
Discosphaera tubifera	*Other*
Emiliania huxleyi	*Emiliania huxleyi*
Florisphaera profunda	*Other*
Gaarderia corolla	*Other*
Gephyrocapsa ericsonii	*Gephyrocapsa oceanica*
Gephyrocapsa oceanica	*Gephyrocapsa oceanica*
Helicosphaera wallichii	*Other*
Helladosphaera cornifera ?	*Other*
Michaelsarsia elegans	*Others*
Ophiaster formosus	*Ophiaster* spp.
Ophiaster hydroideus	*Ophiaster* spp.
Ophiaster reductus	*Ophiaster* spp.
Palusphaera Vandelii	*Others*
Pappomonas spp.	*Other*
Polygrater sp *?*	*Other*
Rhabdosphaera Clavigera	*Other*
Syracosphaera spp.	*Syracosphaera* spp.
Syracosphaera corolla	*Syracosphaera* spp.
Syracosphaera lamina	*Syracosphaera* spp.
Syracosphaera molischii	*Syracosphaera* spp.
Syracosphaera nana	*Syracosphaera* spp.
Syracosphaera nodosa	*Syracosphaera* spp.
Syracosphaera noroitica	*Syracosphaera* spp.
Syracosphaera prolongata	*Syracosphaera* spp.
Syracosphaera pulchra	*Syracosphaera* spp.
Syracosphaera rotula	*Syracosphaera* spp.
Umbellosphaera irregularis	*Umbellosphaera irregularis*
Umbilicosphaera hulburtiana	*Umbilicosphaera* spp.
Umbilicosphaera sibogae	*Umbilicosphaera* spp.

References

Anderson, J., Samoilys, M., 2016. The small pelagic fisheries of Tanzania. In: Anderson, J., Andrew, T. (Eds.), Case Studies on Climate Change and African Coastal Fisheries: a Vulnerability Analysis and Recommendations for Adaptation Options, Rome, Italy, FAO. Fisheries and Aquaculture Circular No, vol. 1113, pp. 19–59.

Bakun, A., Roy, C., Lluch-Cota, S., 1998. Coastal upwelling and other processes regulating ecosystem productivity and fish production in the Western Indian Ocean. In: Sherman, K., Okemwa, E.N., Ntiba, M.J. (Eds.), Large Marine Ecosystems of the Indian Ocean: Assessment, Sustainability, and Management. Blackwell Science, Malden, MA, pp. 103–141.

Barlow, R., Lamont, T., Kyewalyanga, M., Sessions, H., van den Berg, M., Duncan, F., 2011. Phytoplankton production and adapation in the vicinity of Pemba and Zanzibar islands, Tanzania. Afr. J. Mar. Sci. 33 (2), 283–295.

Bryceson, I., 1977. An ecological study of the phytoplankton of the coastal waters of Dar es Salaam. University of Dar es Salaam PhD thesis, p. 560 pages.

Bryceson, I., 1982. Seasonality of oceanographic conditions and phytoplankton in Dar es Salaam waters. University Science Journal (University of Dar es Salaam) 8 (1&2), 66–76.

Cros, L., Fortuno, J.-M., 2002. Atlas of Northwestern Mediterranean coccolithophores. Sci. Mar. 66 (S1), 1–186.

Cushing, D.H., 1973. Production in the Indian Ocean and the transfer from the primary to the secondary level. In: Zeitschel, B. (Ed.), The Biology of the Indian Ocean. Chapman and Hall, London, pp. 475–486.

Daniel, A., Kerouel, R., Aminot, A., 2012. Pasteurization: a reliable method for preservation of nutrient in seawater samples for inter-laboratory and field applications. Mar. Chem. 128–129, 57–63.

Durak, G.M., Taylor, A.R., Walker, C.E., Probert, I., de Vargas, C., Audic, S., Schroeder, D., Brownlee, C., Wheeler, G.L., 2016. A role for diatom-like silicon transporters in calcifying coccolithophores. Nat. Commun. 7, 10543. https://doi.org/10.1038/ncomms10543.

Fryxell, G.A., 2000. *Nitzschia bicapitata* (bacillariophyceae) and related taxa from oceanic aggregations. Diatom Research 15 (1), 43–73. https://doi.org/10.1080/0269249X.0262000.9705486.

Fryxell, G.A., Hasle, G.R., 2004. Taxonomy of harmful marine diatoms. Manual on Harmful Marine Microalgae, Second Ed. UNESCO Publishing, Paris, pp. 465–509.

GEF/TWAP, 2015. LME 31 - Somali Coastal Current. UNEP, Nairobi, Kenya. **https://geftwap.org**. (Accessed 7 January 2019).

Hallegraeff, G.M., 2004. Harmful algal blooms: a global overview. In: Manual on Harmful Marine Microalgae, Second Ed. UNESCO Publishing, Paris, pp. 25–49.

Hansen, G., Turquet, J., Quod, J.P., Ten-Hage, L., Lugomela, C., Kyewalyanga, M., Hurbungs, M., Wawiye, P., Ogongo, B., Tunje, S., Rakotoarinjanahary, H., 2001. Potentially Harmful Microalgae of the Western Indian Ocean - a Guide Based on a Preliminary Survey. IOC Manuals and Guides No. 41. UNESCO, p. 108.

Hansman, R.L., Sessions, A.L., 2016. Measuring thein situcarbon isotopic composition of distinct marine plankton populations sorted by flow cytometry. Limnol Oceanogr. Methods 14 (2), 87–99.

Hartnoll, R.G., 1974. The Kunduchi marine biology station. Tanzan. Notes Rec. 74, 39–47.

Harvey, J., 1977. Some aspects of the hydrography of the water off the coast of Tanzania: a contribution to CINCWIO. University Science Journal (University of Dar Es Salaam) 3 (1 & 2), 53–92.

Hasle, G.R., Syvertsen, E.E., 1997. Marine diatoms. In: Tomas, C.R. (Ed.), Identifying Marine Phytoplankton. Academic Press, San Diego, pp. 5–385.

Holte, J., Talley, L.D., Gilson, J., Roemmich, D., 2017. An Argo mixed layer climatology and database. Geophys. Res. Lett. 44, 5618–5626. https://doi.org/10.1002/2017GL073426.

Holte, J., Talley, L., 2009. A new algorithm for finding mixed layer depths with applications to Argo data and Subantarctic mode water formation. J. Atmos. Ocean. Technol. 26, 1920–1939.

Hoover, R.S., Hoover, D., Miller, M., Landry, M.R., DeCarlo, E.H., Mackenzie, F.T., 2006. Zooplankton response to storm runoff in a tropical estuary: bottom-up and top-down controls. Mar. Ecol. Prog. Ser. 318, 187–201.

Hopkins, J., Henson, S.A., Painter, S.C., Tyrrell, T., Poulton, A.J., 2015. Phenological characteristics of global coccolithophore blooms. Global Biogeochem. Cycles 29, 239–253. https://doi.org/10.1002/2014GB004919.

Huggett, J.A., 2014. Mesoscale distribution and community composition of zooplankton in the Mozambique Channel. Deep Sea Res. Part II 100, 119–135.

Huggett, J.A., Kyewalyanga, M., 2017. In: Groeneveld, J.C., Koranteng, K.A. (Eds.), Ocean Productivity *in* the RV Dr Fridtjof Nansen in the Western Indian Ocean: Voyages of Marine Research and Capacity Development. FAO, pp. 55–80.

Hydes, D.J., Aoyama, M., Aminot, A., Bakker, K., Becker, S., Coverly, S., Daniel, A., Dickson, A.G., Grosso, O., Kerouel, R., van Ooijen, J., Sato, K., Tanhua, T.,

Woodward, E.M.S., Zhang, J.Z., 2010. Determination of Dissolved Nutrients (N, P, Si) in Seawater with High Precision and Inter-comparability Using Gas-Segmented Continuous Flow Analysers. The GO-Ship Repeat Hydrography Manual: A Collection of Expert Reports and Guidelines, IOCCP Report No. 14, ICPO Publication Series No. 134. Version 1, 2010, pp. 1–87.

Iversen, S.A., Myklevoll, S., Lwiza, K., Yonazi, J., 1984. Tanzanian marine fish resources in the depth region 10–500 m investigated by R/V "DR. FRIDTJOF NANSEN": bergen, Norway, Institute of Marine Research, p. 45–83. In: Iversen, S.A., Myklevoll, S. (Eds.), The Proceedings of the NORAD/Tanzania Seminar to Review the Marine Fish Stocks and Fisheries in Tanzania, Held at Mbegani. Tanzania 6–8 March 1984.

Jebri, F., Jacobs, Z.L., Raitsos, D.E., Srokosz, M., Painter, S.C., Kelly, S., Roberts, M.J., Scott, L., Taylor, S.F.W., Palmer, M., Kizenga, H., Shaghude, Y., Wihsgott, J., Popova, E., 2020. Interannual monsoon wind variability as a key driver of East African small pelagic fisheries. Sci. Rep. 10 (1), 13247. https://doi.org/10.1038/s41598-020-70275-9.

Kirk, J.T.O., 2010. In: Light and Photosynthesis in Aquatic Ecosystems, Third Ed. Cambridge University Press, Cambridge, p. 649.

Kromkamp, J., De Bie, M., Goosen, N., Peene, J., Van Rijswijk, P., Sinke, J., Duineveld, G. C.A., 1997. Primary production by phytoplankton along the Kenyan coast during the SE monsoon and November intermonsoon 1992, and the occurrence of *Trichodesmium*. Deep Sea Res. Part II 44 (6–7), 1195–1212.

Kyewalyanga, M., Lugomela, C., 2001. Existence of potentially harmful microalgae in coastal waters around Zanzibar: a need for a monitoring programme? In: Richmond, M.D., Francis, J. (Eds.), Marine Science Development in Tanzania and Eastern Africa. Proceedings of the 20th Aniversary Conference on Advances in Marine Sciences in Tanzania. IMS/WIOMSA, Zanzibar, pp. 319–328.

Lee, H.Y., Fryxell, G.A., 1996. Bicapitate Nitzschia species: abundant nanoplankton in aggregates during November-December (1992) in the equatorial Pacific. Journal of Plankton Research 18 (8), 1271–1294.

Leetmaa, A., 1972. The response of the Somali current to the southwest monsoon of 1970. Deep Sea Res. 19, 319–325.

Legendre, P., Legendre, L., 1998. Numerical Ecology, 2nd Edition. Elsevier.

Lugomela, C., 1996. Studies of phytoplankton in the nearshore waters of Zanzibar. MSc thesis, University of Dar es Salaam.

Lugomela, C., 2013. Population dynamics of *Pseudo-Nitzschia* species (Bacillariophyceae) in the near shore waters of Dar es Salaam, Tanzania. Tanzan. J. Sci. 39, 38–48.

Lugomela, C., Lyimo, T.J., Bryceson, I., Semsei, A.K., Bergman, B., 2002. *Trichodesmium* in coastal waters of Tanzania: diversity, seasonality, and nitrogen and carbon fixation. Hydrobiologia 477, 1–13.

Lugomela, C.V., Semesi, A.K., 1996. Spatial and temporal variations of phytoplankton in Zanzibar near shore waters. In: Bjork, M., Semesi, A.K., Pedersen, M., Bergman, B. (Eds.), Current Trends in Marine Botanical Research in the East African Region. Sida/SAREC, Stockholm, pp. 235–251.

Lyimo, T.J., 2011. Distribution and abundance of the cyanobacterium *Richelia intracellularis* in the coastal waters of Tanzania. Journal of Ecology and the Natural Environment 3 (3), 85–94.

Magurran, A.E., 2004. Measuring Biological Diversity. Blackwell Science, Malden, MA, p. 256.

McClanahan, T.R., 1988. Seasonality in East Africa's coastal waters. Mar. Ecol. Prog. Ser. 44, 191–199.

Mengesha, S., Dehairs, F., Elskens, M., Goeyens, L., 1999. Phytoplankton nitrogen nutrition in the western Indian Ocean: ecophysiological adaptations of neritic and oceanic assemblages to ammonium supply. Estuar. Coast Shelf Sci. 48, 589–598.

Mgaya, Y.D., 2000. Other Marine Living Resources. In: Ngusaru, A.S. (Ed.), The Present State of Knowledge of Marine Science in Tanzania: Synthesis Report. Tanzania Coastal Management Partnership, Dar es Salaam, Tanzania, pp. 166–182. https://www.crc.uri.edu/download/2001_5047_TCMP_Knowledge.pdf.

Montoya, J.P., 2008. Nitrogen stable isotopes in marine environments. In: Capone, D.G., Bronk, D.A., Mulholland, M.R., Carpenter, E.J. (Eds.), Nitrogen in the Marine Environment, Second Ed. Academic Press, pp. 1277–1302 https://doi.org/10.1016/B978-0-12-372522-6.00029-3.

Moto, E., Kyewalyanga, M., Lyimo, T., Hamisi, M., 2018. Species composition, abundance and distribution of phytoplankton in the coastal waters off Zanzibar Island, Tanzania. J. Biodivers. Environ. Sci. (JBES) 12 (5), 108–119.

Narciso, Á., Gallo, F., Valente, A., Cachão, M., Cros, L., Azevedo, E.B., Barcelos e Ramos, J., 2016. Seasonal and interannual variations in coccolithophore abundance off Terceira Island, Azores (Central North Atlantic). Continent. Shelf Res. 117, 43–56.

Newell, B.S., 1957. A Preliminary Survey of the Hydrography of the British East African Coastal Waters, vol. 9. East African Marine Fisheries Research Organisation, London, p. 23. Fishery Publications No.

Newell, B.S., 1959. The Hydrography of the British East African Coastal Waters, vol. 12. East African Marine Fisheries Research Organisation, London, p. 23. Fishery Publications No.

Noyon, M., Morris, T., Walker, D., Huggett, J., 2019. Plankton distribution within a young cyclonic eddy off south-western Madagascar. Deep Sea Res. Part II 166, 141–150.

Obura, D., Burgener, V., Owen, S., Gonzales, A., 2017. Reviving the Western Indian Ocean Economy: Actions for a Sustainable Future. WWF International, Gland, Switzerland, p. 64.

Oksanen, J., Blanchet, F.G., Friendly, M., Kindt, R., Legendre, P., McGlinn, D., Minchin, P.R., O'Hara, R.B., Simpson, G.L., Solymos, P., Henry, M., Stevens, H., Szoecs, E., Wagner, H., 2019. vegan: community Ecology Package. R package version 2.5-6. https://CRAN.R-project.org/package=vegan.

Painter, S.C., 2020. The biogeochemistry and oceanography of the east african coastal current. Prog. Oceanogr. 186, 102374. https://doi.org/10.101016/j.pocean.102020.102374.

Painter, S.C., Sanders, R., Waldron, H.N., Lucas, M.I., Torres-Valdes, S., 2008. Urea distribution and uptake in the Atlantic Ocean between 50°N and 50°S. Mar. Ecol. Prog. Ser. 368, 53–63. https://doi.org/10.3354/meps07586.

Painter, S.C., Patey, M.D., Tarran, G.A., Torres-Valdes, S., 2014. Picoeukaryote distribution in relation to nitrate uptake in the oceanic nitracline. Aquat. Microb. Ecol. 72, 195–213. https://doi.org/10.3354/ame01695.

R Core Team, 2016. R: A Language and Environment for Statistical Computing. R Foundation for Statistical Computing, Vienna, Austria. URL. https://www.R-project.org/.

Ranaivoson, L.R., Magazzu, G., 1996. The Picoplankton Contribution to the Primary Production on the Northwest Coast of Madagascar. Current Trends in Marine Botanical Research in the East African Region: Proceedings of the 3-10 December 1995 Symposium on the Biology of Microalgae, Macroalgae and Seagrasses in the Western Indian Ocean. University of Mauritius, Mauritius.

Rau, G.H., Sweeney, R.E., Kaplan, I.R., 1982. Plankton ^{13}C:^{12}C ratio changes with latitude:differences between northern and southern oceans. Deep Sea Res. 29 (8A), 1035–1039.

Roberts, M.J., Ribbink, A.J., Morris, T., Duncan, F., Barlow, R., Kaehler, S., Huggett, J., Kyewalyanga, M., Harding, R., van den Berg, M., 2008. 2007 Western Indian Ocean Cruise and Data Report: ALG160. Grahamstown. African Coelacanth Ecosystem Programme, South Africa.

Round, F.E., Crawford, R.M., Mann, D.G., 1990. The Diatoms: Biology and Morphology of the genera. Cambridge University press, UK, p. 747.

Saino, T., Hattori, A., 1980. ^{15}N natural abundance in oceanicsuspended particulate matter. Nature 283, 752–754.

Schott, F.A., McCreary Jr., J.P., 2001. The monsoon circulation of the Indian Ocean. Prog. Oceanogr. 51, 1–123.

Scott, L.E.P., 2004. Information Management and Environmental Education Report: ACEP Seventh Expedition ALG 130. *African Coelacanth Ecosystem Programme*, Technical Report. Grahamstown, South Africa.

Sekadende, B., Scott, L., Anderson, J., Aswani, S., Francis, J., Jacobs, Z., Jebri, F., Jiddawi, N., Kamukuru, A.T., Kelly, S., Kizenga, H., Kuguru, B., Kyewalyanga, M., Noyon, M., Nyandwi, N., Painter, S.C., Palmer, M., Raitsos, D.E., Roberts, M., Sailley, S.F., Samoilys, M., Sauer, W.H.H., Shayo, S., Shaghude, Y., Taylor, S.F.W., Wihsgott, J., Popova, E., 2020. The small pelagic fishery of the Pemba Channel, Tanzania: what we know and what we need to know for management under climate change. Ocean Coast Manag. 197, 105322 https://doi.org/10.1016/j.ocecoaman.102020.105322.

Semba, M., Lumpkin, R., Kimirei, I., Shaghude, Y., Nyandwi, N., 2019. Seasonal and spatial variation of surface current in the Pemba Channel, Tanzania. PloS One 14 (1), e0210303. https://doi.org/10.1371/journal.pone.0210303.

Stolz, K., Baumann, K.-H., Mersmeyer, H., 2015. Extant coccolithophores from the western equatorial Indian Ocean off Tanzania and coccolith distribution in surface sediments. Micropaleontology 61 (6), 473–488.

Swallow, J.C., Schott, F., Fieux, M., 1991. Structure and transport of the East African Coastal Current. J. Geophys. Res. 96 (C12), 22,245-222,257.

Taylor, S.F.W., Roberts, M.J., Milligan, B., Ncwadi, R., 2019. Measurment and implications of marine food security in the Western Indian Ocean: an impending crisis? Food Security 11, 1395–1415, 10.1007/s12571-019-00971-6.

UNEP, 2015. The Regional State of the Coast Report: Western Indian OceanNairobi, Kenya. UNEP and WIOMSA, p. 546.

Unep-Wcmc, W.C., WorldFish Centre, 2010. Global distribution of warm-water coral reefs, compiled from multiple sources including the Millennium Coral Reef Mapping Project. Version 4.0. Includes contributions from IMaRS-USF and IRD (2005), IMaRS-USF (2005) and Spalding et al., (2001). UNEP World Conservation Monitoring Centre, Cambridge (UK). URL: http://data.unep-wcmc.org/datasets/1.

UNESCO, 1981. The Practical Salinity Scale 1978 and the International Equation of State of Seawater 1980. UNESCO Technical Papers in Marine Science, vol. 36. UNESCO, Paris, p. 25.

UNESCO, 2010. The international thermodynamic equation of seawater - 2010: calculation and use of thermodynamic properties. International Oceanographic Commission 171.

van der Elst, R., Everett, B., Jiddawi, N., Mwatha, G., Afonso, P.S., Boulle, D., 2005. Fish, Fishers and fisheries of the Western Indian Ocean: their diversity and status. A preliminary assessment. Philosophical Transactions of the Royal Society A 363, 263–284.

Van der Elst, R.P., Everett, B.I., 2015. Offshore Fisheries of the Southwest Indian Ocean: Their Status and the Impact on Vulnerable Species, vol. 10. Oceanographic Research Institute, Special Publication No., p. 448

van der Lingen, C., Bertrand, A., Bode, A., Brodeur, R., Cubillos, L.A., Espinoza, P., Friedland, K., Garrido, S., Irigoien, X., Miller, T., Möllmannm, C., Rodriguez-Sanchez, R., Tanaka, H., Temming, A., 2009. Trophic dynamics. In: Checkley, D., Alheit, J., Oozeki, Y., Roy, C. (Eds.), Climate Change and Small Pelagic Fish. Cambridge University Press, Cambridge, UK, pp. 112–157.

Venrick, E.L., 1982. Phytoplankton in an oligotrophic ocean: Observations and questions. Ecological Monographs 52 (2), 129–154.

Venrick, E.L., 1990. Phytoplankton in an oligotrophic ocean: Species structure and interannual variability. Ecology 71 (4), 1547–1563.

Venrick, E.L., 1997. Comparison of the phytplankton species composition and structure in the Climax area (1973-1985) with that of station ALOHA (1994). Limnology and Oceanography 42 (7), 1643–1648.

Welschmeyer, N.A., 1994. Fluorometric analysis of chlorophyll a in the presence of chlorophyll b and phaeopigments. Limnol. Oceanogr. 39 (8), 1985–1992.

Wickstead, J.H., 1962. Plankton from the East African area of the Indian Ocean. Nature 162, 1224–1225.
Wickstead, J.H., 1963. Estimates of total zooplankton in the zanzibar area of the Indian Ocean with a comparison of the results with two different nets. Proceedings of the Zoological Society of London 141, 577–608.
Wyrtki, K., 1973. Physical oceanography of the Indian ocean. In: Zeitzschel, B. (Ed.), The Biology of the Indian Ocean. Chapman and Hall, London, pp. 18–36.
Young, J., Geisen, M., Cros, L., Kleijne, A., Sprengel, C., Probert, I., Østergaard, J., 2003. A guide to extant coccolithophore taxonomy. Journal of Nannoplankton Research Special Issue (1), 1–125.
Zubkov, M.V., Fuchs, B.M., Tarran, G.A., Burkhill, P.H., Amann, R., 2003. High rate of uptake of organic nitrogen compounds by *Prochlorococcus* cyanobacteria as a key to their dominance in oligotrophic oceanic waters. Appl. Environ. Microbiol. 69 (2), 1299–1304.